Joint Angle and Delay Estimation for 3D Massive MIMO Systems Based on Parametric Channel Modeling

By

Yan Li

Submitted to the Electrical Engineering and Computer Science Department and the Graduate Faculty of the University of Kansas
in partial fulfillment of the requirements for the degree of
Master of Science

Dr. Lingjia Liu, Chairperson

Committee members

Dr. Erik Perrins

Dr. Shannon Blunt

Date defended: December 2, 2015

The Dissertation Committee for Yan Li certifies
that this is the approved version of the following dissertation :

Joint Angle and Delay Estimation for 3D Massive MIMO Systems Based on Parametric Channel Modeling

Dr. Lingjia Liu, Chairperson

Date approved: December 2, 2015

Abstract

Mobile data traffic is predicted to have an exponential growth in the future. In order to meet the challenge as well as the form factor limitation on the base station, 3D “massive MIMO" has been proposed as one of the enabling technologies to significantly increase the spectral efficiency of a wireless system. In “massive MIMO" systems, a base station will rely on the uplink sounding signals from mobile stations to figure out the spatial information to perform MIMO beam-forming. Accordingly, multi-dimensional parameter estimation of a MIMO wireless channel becomes crucial for such systems to realize the predicted capacity gains.

In this thesis, we study and analyze both separated and joint angle and delay estimation for 3D “massive MIMO" systems based on parametric channel modeling in mobile wireless communications. To be specific, we first introduce a separated low complexity time delay and angle estimation in the millimeter wave massive MIMO system. Furthermore, a matrix-based ESPRIT-type algorithm is applied to jointly estimate delay and angle, the mean square error (MSE) of which is also analyzed. We found that azimuth estimation depends on the number of vertical antenna elements as well as that of horizontal antenna elements. Simulation results suggest that the configuration of the underlying antenna at the base station plays a critical role in determining the estimation performance. These insights will be useful for designing practical “massive MIMO" systems in future mobile wireless communications.

Acknowledgements

I would like to express my deepest gratitude to my advisor, Dr. Lingjia Liu for his support of my master study and research, for his patience, motivation and immense knowledge. His guidance always accompanies with me in all the time of research and writing this thesis. Besides my advisor, I wish to thank Dr. Erik Perrins, Dr. Shannon Blunt for their time to serve on my committee and provide the helpful advice. I would like to extend my thanks to all my friends in University of Kansas for their help. Last but not the least, I would like to thank my mother and father for their encouragement, support and understanding.

Contents

List of Figures

Chapter 1

Introduction

Rarely have technical innovations changed everyday lift as rapidly and profoundly as mobile wireless communications. According to the International Telecommunication Union (ITU) [1], the number of mobile wireless subscriptions has passed 6.83 billion in year 2013, which is more than 90% of the world population. In additional, smart phone and mobile tablet penetrations are also rising rapidly. In general, the data consumption of a single smart phone is equivalent to the traffic generated by 50 featured phones; while a mobile tablet can produce 120 times the data volume of a featured phone [2]. As a result, in May 2013, Cisco systems predicted a staggering 66% compound annual growth rate (CAGR) for global mobile data traffic from 2012 to 2017 [3]. This is an 13-fold increase in wireless traffic over a five-year period.

A key societal question and a pressing engineering challenge is:"How can we support the predict exponential growth in mobile data traffic?" To meet the increasing traffic demand, other than reallocating radio spectrum to wireless providers, spectrum efficiency will need to be improved significantly. Multiple-input-multiple-output (MIMO) technology, together with multi-user MIMO (MU-MIMO), offer efficient ways to increase the spectral efficiency of a mobile broadband communication system [4]. Recently, a new MIMO paradigm called "Massive MIMO" has generated much interest in both academia [5] [6] and industry. Using information theoretical analysis, it can be shown that even with random user scheduling and no inter-cell cooperation, unprecedented

spectral efficiency in time-division-duplex (TDD) cellular systems can be achieved if a sufficiently large number of transmit antennas are employed at each base station.

Due to the form factor limitation, 3D "massive MIMO" systems are introduced to fit a large number of antenna elements on the base station in reality [7] [8]. On the other side, millimeter wave wireless communication with carrier frequency between 30 to 300GHz has enable gigabit per second data transmission indoor wireless communication systems and has been introduced for mobile cellular network to combat the form factor limitation. Communication in the millimeter wave band make it possible to pack a large amount of antenna elements on a base station therefore also enable practical massive MIMO systems.

In order to realized the capacity gains promised by "massive MIMO" systems, it is crucial for the base station to know the channel state information (CSI) to perform the transmit precoding. Traditionally, channel estimation can be done by estimating the transfer function. Such a strategy may yield poor performance in 3D active "massive MIMO" systems due to the large dimensionality of the channel matrix. Alternatively, channel estimation could be conducted based on parametric channel models where direction-of-arrival (DoA) and direction-of-departure (DoD) estimation of resolvable paths can be estimated [9]. When the system is calibrated, it is shown that the performance bound of the channel estimation through a parametric approach outperforms simple unstructured interpolation scheme [10]. Under parametric channel modeling of massive MIMO systems, estimation of the channel becomes estimation of the DoA/DoD and the delay of each resolvable paths. In this thesis, we focus on joint angle and delay estimation for 3D massive MIMO systems based on parametric channel modeling.

There are many existing subspace-based method such as MUSIC, ESPRIT and matrix pencil to estimate DoA/DoD for two-dimensional (2D) mobile wireless systems. However, its counterpart in 3D, together with delay estimation is yet not well explored for mobile wireless communication systems. In [11], an efficiency way for estimating the delay and DoA of multiple reflections of a know signal is presented, but the complexity of the algorithm is prohibitively high due to the iterative procedure. Some methods in [12] are introduced to estimate channel parameters with

low complexity, but the disadvantages are that the pairing of the 3D angles and delay can not be automatically determined, which means two signals with closed parameters are indistinguishable. The TST-MUSIC (Time-Space-Time MUSCI) algorithm proposed in [13] has great performance in estimating the DoAs and delay of a wireless multi-ray channel, but it can only solve the problem in the case of only one close parameter and the complexity is still relatively high. Hence, in this thesis, we introduce two approaches to estimate the DoAs and delay with low complexity utilizing the shift-invariance property of ESPRIT algorithm. Moreover, few of the aforementioned papers deal with derivation of the analytical mean square error (MSE). Analytical results on the performance of standard ESPRIT is first investigated in [14]. However, the result goes back to a result on the distribution of the eigenvectors of a simple covariance matrix. In contrast, in [15] a different approach is proposed, which provides an explicit first-order expression of the subspace of a desired signal if a small additive perturbation is assumed. Nevertheless, the authors in [15] only consider the 1D standard ESPRIT method. Moreover, the white noise is assumed in order to get the desired result. In order to overcome these drawbacks, Roemer *et.al* [16] provider a frame of the MSE analysis which considers the multiple dimensions case. In [16], it is shown that the MSE expression only depends on the second-order moments of the noise. However, these results are so complicated and only can be simplified in the signal path case. Thus little intuition can be obtained through them. In this thesis, we will derive the simplified results in multiple paths case using the subspace-based estimation methods in the millimeter wave massive MIMO system, which can provide us the intuitions of the real system designing.

The contribution of the thesis can be summarized as follows.

Firstly, we propose the separated delay and angle estimation method, which is rarely investigated in the literature. It has also been shown that if DoAs of different paths are drawn to uniform distribution, the delays of different paths can be estimated correctly and vice versa.

Secondly, we derive the MSE of the delay and angle estimation for different paths using the standard and unitary ESPRIT. Furthermore, we simplify the results in the massive MIMO system which shows that the MSE depends heavily on the number of the antennas, the number of the

snapshots and the transmit power. There are few papers focusing on the analysis of the MSE of the elevation angle and azimuth angle estimation for different paths. Compared to the results in the literature, our analytical result can provide the intuitions of the real system design.

Thirdly, we analyze the impact of various antenna configurations on the estimation performance and observe some "surprising" results. For example, for a system with total 64 antenna elements, using ESPRIT-type DoA estimation algorithms, it can be shown that a 8×8 array yields better DoA estimation than 4×16 array in both elevation angle and azimuth angle estimation in the low and median signal to noise ratio (SNR) regime.

Finally, the MSE of the delay and angle estimation using joint angle and delay estimation (JADE) methodology is investigated. In the massive MIMO system, the simplified closed-form MSE of elevation angle and azimuth angle estimation is obtained, which is unexplored in the literature.

The remainder of this thesis is organized as follows. We introduce the multi-path ray-based channel model in Chapter 2. Chapter 3.1 mainly focuses on delay estimation based on discrete Fourier transform, while the 3D DoA estimation following our line of work is given in Chapter 3.2 through unitary ESPRIT. The matrix-based joint angle and delay estimation algorithm is conducted in Chapter 4.1, together with the theoretical analysis of the mean square error (MSE) of the proposed method in Chapter 4.2. Simulation results are illustrated in Chapter 5. Finally, Chapter 6 concludes this thesis and we show a list of active research topics which need to be investigated in the future.

Chapter 2

Data Model

A typical 3D "massive MIMO" system with $M \times N$ antenna array at the base station can be shown in Fig. 2.1.

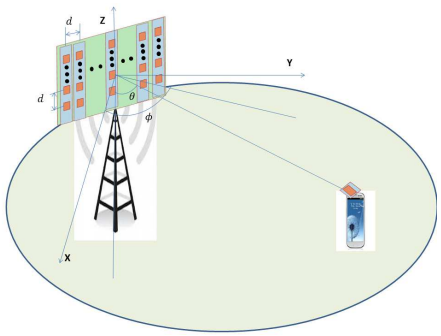

Figure 2.1: Model of 3D “Massive MIMO” System

In this particular system, a base station is at the height of h, while a mobile station is at the height of h_m. The antenna array at the base station is a planar array placed in the X-Z plane with M antenna elements vertically and N antenna elements horizontally. The spacing between adjacent antenna element is assumed to be d. For simplicity, throughout the thesis, we assume that there is only one transmit antenna at the mobile station. In the 3D communication system shown in Fig. 2.1, instead of mechanical down-tiling the antenna array towards the mobile station, the base station could also perform digital beam-forming in both elevation and azimuth domain towards the mobile station. In TDD system, 3D direction of arrival estimation will provide the base station the channel

knowledge on the downlink. That is why it is crucial for TDD based "massive MIMO" system. In reality, the propagation situation in a wireless communication system is rather complicated. The uplink sounding reference signals usually go through scattering, reflection and diffraction before they reach the base station. For a multiple path scenario, a 3D wireless channel is usually modeled by a finite number of rays, each parameterized by a complex amplitude, angle and time delay [10].

Generally, suppose that there are P resolvable propagation paths impinging on a R-dimensional grid of size $M_1 \times M_2 \cdots \times M_R$ [17], the measurement data samples are given by:

$$y_{m_1,m_2,\ldots,m_R}(t) = \sum_{\ell=1}^{P} \alpha_\ell(t) \prod_{r=1}^{R} e^{j(m_r-1)u_\ell^{(r)}} r(t-\tau_\ell) + w_{m_1,m_2,\ldots,m_R}(t), \tag{2.1}$$

where $m_r = 1,2,\ldots,M_r$. $\alpha_\ell(t)$ denotes the complex channel gain of ℓ-th path at time instant t. $u_\ell^{(r)}$ symbolizes the spatial frequency of path ℓ in the r-th mode for $r = 1,2,\ldots,R$. $r(t)$ is the transmitted signal, denoted by $r(t) = \sum_k s_k g(t-kT)$, where s_k is the sequence of data bits we transmitted over the channel, and $g(t)$ is a known pulse shape function by which s_k is modulated. T is the symbol rate and for notation simplicity, it will be normalized to $T = 1$ from now on. τ_ℓ represents the time delay of path ℓ and $w_{m_1,m_2,\ldots,m_R}(t)$ is assumed to be the zero mean additive Gaussian noise uncorrelated in all dimensions with variance σ^2.

Here, our received signal is referenced by $R+1$ indices and the most common way to handle this multi-dimensional measurement data is to stack dimensions into a highly structured matrix in a majority of existing literatures. In this thesis, our goal is to jointly estimate the 3D DoAs and the corresponding delay of a particular path under a uniform planar array of size $M \times N$. Hence, we will take $R = 2$ to introduce the matrix-based system model.

Accordingly, (2.1) implies that the received signal impinging on a 2D antenna array can be compactly expressed as:

$$\mathbf{Y}(t) = \sum_{\ell=1}^{P} \alpha_\ell(t)\mathbf{a}(u_\ell)\mathbf{a}^T(v_\ell)r(t-\tau_\ell) + \mathbf{W}(t), \tag{2.2}$$

where $\mathbf{a}(u_\ell) = \begin{bmatrix} 1 & e^{ju_\ell} & \dots & e^{j(M-1)u_\ell} \end{bmatrix}^T$ and $\mathbf{a}(v_\ell) = \begin{bmatrix} 1 & e^{jv_\ell} & \dots & e^{j(N-1)v_\ell} \end{bmatrix}^T$ can be viewed as the steering vector of elevation angle and azimuth angle respectively. $u_\ell = \frac{2\pi d}{\lambda}\cos\theta_\ell$, $v_\ell = \frac{2\pi d}{\lambda}\sin\theta_\ell\cos\phi_\ell$ represent two spatial frequencies of path ℓ, λ is the wavelength. $\mathbf{W}(t)$ denotes the AWGN noise and each of its element has zero mean and variance σ^2, $\alpha_\ell(t)$ is the channel gain of the ℓ-th path.

Now we need to stack dimensions through collecting all array responses into an $M \times N$ steering matrix $\mathbf{A}(u_\ell, v_\ell)$, it can be shown that:

$$\mathbf{a}_\ell = \mathbf{a}(v_\ell) \otimes \mathbf{a}(u_\ell),$$

where $\otimes$ is the Kronecker product.

We can construct a 2D steering matrix of the received signal, $\mathbf{A} = \begin{bmatrix} \mathbf{a}_1 & \mathbf{a}_2 & \dots & \mathbf{a}_P \end{bmatrix} \in \mathbb{C}^{MN\times P}$ based on $\mathbf{a}_\ell$, which contains all the information related to the P paths signal whose elevation angle θ_ℓ and azimuth angle ϕ_ℓ are to be estimated.

It is reasonable to assume that the known modulation pulse shape function $g(t)$ has finite support $[0, L_g)$ and the channel is fading but stationary over short time intervals. With $\tau_{max} = \max_{1\le\ell\le P}\tau_\ell$ denotes the maximum delay spread, the channel length is $L = L_g + \tau_{max}$, which means the channel impulse response $\mathbf{h}^{(n)}(t)$ in the n-th time interval has finite duration and is zero outside an interval $[0, L)$ [18]:

$$\mathbf{h}^{(n)}(t) = \sum_{\ell=1}^{P} \alpha_\ell^{(n)}(t)\mathbf{a}_\ell g(t-\tau_\ell) \tag{2.3}$$

where L and L_g are both measured in symbol periods. It should be noted that the number of the paths in the millimeter wave system is rather limited [19, 20]. We assumed that the received data is sampled at a rate of V times the symbol rate and we start sampling at $t = nL$. During the first sample period in the n-th time interval, the noiseless received data written in vector form is shown

to be:

$$\begin{bmatrix} \mathbf{y}^{(n)}(0) \\ \mathbf{y}^{(n)}(\frac{1}{V}) \\ \vdots \\ \mathbf{y}^{(n)}(1-\frac{1}{V}) \end{bmatrix} = \mathbf{H}^{(n)} \begin{bmatrix} s_0^{(n)} \\ s_{-1}^{(n)} \\ \vdots \\ s_{-(L-1)}^{(n)} \end{bmatrix}$$

where

$$\mathbf{H}^{(n)} = \begin{bmatrix} \mathbf{h}^{(n)}(0) & \mathbf{h}^{(n)}(1) & \dots & \mathbf{h}^{(n)}(L-1) \\ \mathbf{h}^{(n)}(\frac{1}{V}) & \mathbf{h}^{(n)}(1+\frac{1}{V}) & \dots & \mathbf{h}^{(n)}(L-1+\frac{1}{V}) \\ \vdots & \vdots & \vdots & \vdots \\ \mathbf{h}^{(n)}(1-\frac{1}{V}) & \mathbf{h}^{(n)}(2-\frac{1}{V}) & \dots & \mathbf{h}^{(n)}(L-\frac{1}{V}) \end{bmatrix}.$$

Extending to Q symbol periods, we obtain the data mode as:

$$\mathbf{Y}_1^{(n)} = \mathbf{H}^{(n)}\mathbf{S}^{(n)} + \mathbf{W}_1^{(n)}, \tag{2.4}$$

where $\mathbf{Y}_1^{(n)}$ represents the $MNV \times Q$ received data matrix and $\mathbf{W}_1^{(n)}$ denotes the AWGN noise. $\mathbf{S}^{(n)}$ is the $L \times Q$ Toeplitz matrix of data symbols. If transmitted sequence $\{s_k^{(n)}\}$ is known, we can directly estimate the $MNV \times L$ channel matrix through least-square type of methods, i.e., $\mathbf{Y}_2^{(n)} = \mathbf{Y}_1^{(n)}\mathbf{S}^{(n)\dagger}$, where the superscript † represents matrix pseudo-inverse. If the transmitted sequence is unknown, the blind channel estimation methodology can be adopted which is beyond the scope of our thesis. In fact, we can always express the noisy channel estimates $\mathbf{Y}_2^{(n)}$ as:

$$\mathbf{Y}_2^{(n)} = \mathbf{H}^{(n)} + \mathbf{W}_2^{(n)}, \tag{2.5}$$

where $\mathbf{W}_2^{(n)} = \mathbf{W}_1^{(n)}\mathbf{S}^{(n)\dagger}$ is the estimation noise matrix.

It is convenient to rearrange the impulse response samples into an $MN \times LV$ channel matrix $\mathbf{H}_v^{(n)}$, which includes all the effects of the array response, path delay, symbol waveform and fading

parameters:

$$\mathbf{H}_v^{(n)} = \begin{bmatrix} \mathbf{a}_1 & \cdots & \mathbf{a}_P \end{bmatrix} \begin{bmatrix} \alpha_1(n) & & \\ & \ddots & \\ & & \alpha_P(n) \end{bmatrix} \begin{bmatrix} \mathbf{g}(\tau_1)^T \\ \vdots \\ \mathbf{g}(\tau_P)^T \end{bmatrix} = \mathbf{A}\text{diag}\{\mathbf{b}(n)\}\mathbf{G}, \tag{2.6}$$

where $\mathbf{b}(n)$ is the $P \times 1$ vector containing complex fading envelope in the n-th time interval. $\mathbf{G}$ denotes the $P \times LV$ time delay matrix, where $\mathbf{g}(\tau_\ell)^T$ is a $1 \times LV$ row vector of samples of $g(t-\tau_\ell)$. In the present of the noise, (2.6) can be expressed as

$$\mathbf{Y}_3^{(n)} = \mathbf{A}\text{diag}\{\mathbf{b}(n)\}\mathbf{G} + \mathbf{W}_3^{(n)}, \tag{2.7}$$

where $\mathbf{W}_3^{(n)}$ is the noise matrix.

Chapter 3

Separated Delay and DoA Estimation

It can be observed from (2.7) that the delay and DoAs can be estimated through the shift-invariance structure of the received signal. In this section, we will introduce the separated delay and DoA estimation algorithm using the standard and unitary ESPRIT method. Furthermore, we will derive the simplified mean square error (MSE) of delay and angle estimation using the standard and unitary ESPRIT method in the millimeter wave massive MIMO system.

3.1 Low Complexity Delay Estimation

It is common to assume that the transmitted waveform function $g(t)$ is the raised cosine roll-off signal. Under the assumption of our data model, the known waveform $g(t)$ is sampled at a rate of V which can be arranged into a row vector:

$$\mathbf{g}^T = \left[\begin{array}{cccc} g(0) & g(\frac{1}{V}) & \dots & g(L-\frac{1}{V}) \end{array} \right]. \tag{3.1}$$

We use a discrete Fourier transform (DFT) to map the delay into phase shift as $\mathbf{g}_F^T = \mathbf{g}^T\mathbf{F}$,

where $\mathbf{F}$ represents the DFT matrix of size $LV \times LV$ defined by [12]:

$$\mathbf{F} = \begin{bmatrix} 1 & 1 & \dots & 1 \\ 1 & e^{-j(2\pi/LV)} & \dots & e^{-j(2\pi/LV)(LV-1)} \\ \vdots & \vdots & & \vdots \\ 1 & e^{-j(2\pi/LV)(LV-1)} & \dots & e^{-j(2\pi/LV)(LV-1)^2} \end{bmatrix}$$

If τ_ℓ is an integer multiple of $1/V$, the Fourier transform $\mathbf{g}_\tau$ of the sampled version of $g(t-\tau)$ is given by

$$\mathbf{g}_\tau = \begin{bmatrix} 1 & \psi^{\tau V} & (\psi^{\tau V})^2 & \dots & (\psi^{\tau V})^{LV-1} \end{bmatrix} \mathrm{diag}(\mathbf{g}_F) \tag{3.2}$$

where $\psi = e^{-j(2\pi/LV)}$.

Under the assumption that $g(t)$ is bandlimited and sampled at or above the Nyquist rate, the channel matrix in (2.6) after DFT transformation can be shown as:

$$\begin{aligned} \mathbf{Y}_4 &= \mathbf{A}\mathrm{diag}\{\mathbf{b}\} \begin{bmatrix} 1 & \psi_1 & \cdots & \psi_1^{LV-1} \\ 1 & \psi_2 & \cdots & \psi_2^{LV-1} \\ \vdots & \vdots & \vdots & \vdots \\ 1 & \psi_P & \cdots & \psi_P^{LV-1} \end{bmatrix} \mathrm{diag}\{\mathbf{g}_F\} + \mathbf{W}_4 \\ &= \mathbf{A}\mathrm{diag}\{\mathbf{b}\}\hat{\mathbf{F}}_\psi \mathrm{diag}\{\mathbf{g}_F\} + \mathbf{W}_4 \end{aligned}$$

where $\psi_\ell = e^{jw_\ell}, w_\ell = -\frac{2\pi}{L}\tau_\ell$. Note that the time index $^{(n)}$ is omitted in this section for brevity.

If $\mathrm{diag}\{\mathbf{g}_F\}$ is non-singular, we can directly estimate the parameter τ_ℓ using standard or unitary ESPRIT after dividing $\mathbf{Y}_4$ by $\mathrm{diag}\{\mathbf{g}_F\}$. However, the matrix $\mathrm{diag}\{\mathbf{g}_F\}$ might be singular because $g(t)$ is a bandlimited signal. Assume that the normalized bandwidth is $W (W < V)$, $\mathbf{g}_F$ only has LW number of non-zero discrete values. In order to avoid blowing up the noise, we need to define a selection matrix $\mathbf{J}_g \in \mathbb{C}^{LV \times LW}$ to choose appropriate submatrices of $\mathbf{Y}_4$. $\mathbf{J}_g$ has the following

form [21]:

$$\mathbf{J}_g = \begin{bmatrix} \mathbf{0} & \mathbf{I}_{\lfloor LW/2 \rfloor} \\ \mathbf{0} & \mathbf{0} \\ \mathbf{I}_{\lceil LW/2 \rceil} & \mathbf{0} \end{bmatrix}. \tag{3.3}$$

We can obtain the channel model with desired structure which is given by:

$$\mathbf{Y}_5 = \mathbf{Y}_4 \cdot \mathbf{J}_g \left[\text{diag}\left\{ \mathbf{g}_F \mathbf{J}_g \right\} \right]^{-1} = \mathbf{A}\text{diag}\left\{ \mathbf{b} \right\} \mathbf{F}_w + \mathbf{W}_5, \tag{3.4}$$

where $\mathbf{W}_5 = \mathbf{W}_4 \cdot \mathbf{J}_g \left[\text{diag}\{ \mathbf{g}_F \mathbf{J}_g \} \right]^{-1}$.

Note that, the role of $\mathbf{F}_w \in \mathbb{C}^{P \times LW}$ is equivalent to the array steering matrix in our former data model [22]. Hence, we can follow our line of work using ESPRIT algorithm to obtain w_ℓ, as well as the parameter of interest τ_ℓ through shift-invariance property.

We can apply the one dimensional standard ESPRIT algorithm to evaluate the estimation performance. Take the transpose of (3.4), we have

$$\begin{aligned} \mathbf{Y}_5^T &= \mathbf{F}_w^T \text{diag}\left\{ \mathbf{b} \right\} \mathbf{A}^T + \mathbf{W}_5^T \\ &= \begin{bmatrix} \mathbf{f}_1 & \mathbf{f}_2 & \dots & \mathbf{f}_P \end{bmatrix} \mathbf{S} + \mathbf{W}_5^T \end{aligned} \tag{3.5}$$

where $\mathbf{f}_\ell = \begin{bmatrix} 1 & e^{jw_\ell} & \dots & e^{j(LV-1)w_\ell} \end{bmatrix}^T$ can be regarded as the steering vector and $\mathbf{S} = \text{diag}\left\{ \mathbf{b} \right\} \mathbf{A}^T$ is the equivalent “training sequence".

In order to estimate the delay of P different paths, the rank of the equivalent “training sequence" $\mathbf{S}$ should be equal to P. In fact, the DoAs of different paths are drawn to the uniform distribution, e.g., $U[-\pi, \pi]$, it can be obtained that the probability that two different paths have the same DoAs is zero. We can easily obtain the rank of the noiseless received signals as follows:

$$\text{Rank}\left\{ \text{diag}\left\{ \mathbf{b}(n) \right\} \mathbf{A}^T \right\} = \text{Rank}\left\{ \text{diag}\left\{ \mathbf{b}(n) \right\} \right\} = P. \tag{3.6}$$

We can also perform one dimensional unitary ESPRIT algorithm which has low computational

complexity. To be specific, the received signal after the forward and backward averaging becomes:

$$\mathbf{Y}_{du} = \begin{bmatrix}\mathbf{Y}_5^T & \mathbf{\Pi}_{LW}\mathbf{Y}_5^H\mathbf{\Pi}_{MN}\end{bmatrix} = \begin{bmatrix}\mathbf{F}_w^T\mathbf{S} & \mathbf{\Pi}_{LW}\mathbf{F}_w^H\mathbf{S}^*\mathbf{\Pi}_{MN}\end{bmatrix} + \begin{bmatrix}\mathbf{W}_5^T & \mathbf{\Pi}_{LW}\mathbf{W}_5^H\mathbf{\Pi}_{MN}\end{bmatrix} \tag{3.7}$$

where $\mathbf{\Pi}_m$ is the exchange matrix which has one on its antidiagonal elements and zeros elsewhere.

It has been proved in [16] that the unitary transformation will not affect the MSE of the ESPRIT method, however, it is clear that the statistics of the noise and the signal subspace are changed due to the forward and backward averaging. The covariance and complementary covariance matrix becomes:

$$\begin{aligned}\mathbf{R}_{nn}^{(fba)} &= \begin{bmatrix}\mathbf{R}_{nn} & \mathbf{0} \\ \mathbf{0} & \mathbf{\Pi}_{LWMN}\mathbf{R}_{nn}^*\mathbf{\Pi}_{LWMN}\end{bmatrix} \\ \mathbf{C}_{nn}^{(fba)} &= \begin{bmatrix}\mathbf{0} & \mathbf{R}_{nn}\mathbf{\Pi}_{LWMN} \\ \mathbf{\Pi}_{LWMN}\mathbf{R}_{nn}^* & \mathbf{0}\end{bmatrix},\end{aligned} \tag{3.8}$$

where $\mathbf{R}_{nn} = \mathbb{E}\left\{\mathrm{vec}\left\{\mathbf{W}_5^T\right\}\mathrm{vec}\left\{\mathbf{W}_5^T\right\}^H\right\}$.

Proof. Denote $\mathbf{n}_{du} = \mathrm{vec}\{\begin{bmatrix}\mathbf{W}_5^T & \mathbf{\Pi}_{LW}\mathbf{W}_5^H\mathbf{\Pi}_{MN}\end{bmatrix}\}$ be the noise vector after forward-backward averaging. Based on the definition of the covariance matrix, we have

$$\begin{aligned}\mathbf{R}_{nn}^{(fba)} &= \mathbb{E}\{\mathbf{n}_{du}\cdot\mathbf{n}_{du}^H\} \\ &= \begin{bmatrix}\mathrm{vec}\left\{\mathbf{W}_5^T\right\} \\ \mathrm{vec}\left\{\mathbf{\Pi}_{LW}\mathbf{W}_5^H\mathbf{\Pi}_{MN}\right\}\end{bmatrix}\begin{bmatrix}\left\{\mathrm{vec}\left\{\mathbf{W}_5^T\right\}\right\}^H & \left\{\mathrm{vec}\left\{\mathbf{\Pi}_{LW}\mathbf{W}_5^H\mathbf{\Pi}_{MN}\right\}\right\}^H\end{bmatrix} \\ &= \begin{bmatrix}\mathrm{vec}\{\mathbf{W}_5^T\}\left\{\mathrm{vec}\{\mathbf{W}_5^T\}\right\}^H & \mathrm{vec}\{\mathbf{W}_5^T\}\left\{\mathrm{vec}\left\{\mathbf{\Pi}_{LW}\mathbf{W}_5^H\mathbf{\Pi}_{MN}\right\}\right\}^H \\ \mathrm{vec}\left\{\mathbf{\Pi}_{LW}\mathbf{W}_5^H\mathbf{\Pi}_{MN}\right\}\left\{\mathrm{vec}\left\{\mathbf{W}_5^T\right\}\right\}^H & \mathrm{vec}\left\{\mathbf{\Pi}_{LW}\mathbf{W}_5^H\mathbf{\Pi}_{MN}\right\}\left\{\mathrm{vec}\left\{\mathbf{\Pi}_{LW}\mathbf{W}_5^H\mathbf{\Pi}_{MN}\right\}\right\}^H\end{bmatrix}\end{aligned}$$

It can be immediately observed that $\mathrm{vec}\{\mathbf{W}_5^T\}\left\{\mathrm{vec}\{\mathbf{W}_5^T\}\right\}^H = \mathbf{R}_{nn}$. In the next step, we can

further simplify the rest entries in the covariance matrix as:

$$\begin{aligned}
&\text{vec}\{\mathbf{W}_5^T\}\left\{\text{vec}\left\{\mathbf{\Pi}_{LW}\mathbf{W}_5^H\mathbf{\Pi}_{MN}\right\}\right\}^H \\
&= \text{vec}\{\mathbf{W}_5^T\}\left\{\mathbf{\Pi}_{LW}\otimes\mathbf{\Pi}_{MN}\text{vec}\left\{\mathbf{W}_5^H\right\}\right\}^H \\
&= \text{vec}\{\mathbf{W}_5^T\}\left\{\mathbf{\Pi}_{MNLW}\text{vec}\left\{\mathbf{W}_5^H\right\}\right\}^H \\
&= \text{vec}\{\mathbf{W}_5^T\}\left\{\text{vec}\left\{\mathbf{W}_5^T\right\}\right\}^T\mathbf{\Pi}_{MNLW} \\
&= \mathbf{0}
\end{aligned}$$

and

$$\begin{aligned}
&\text{vec}\left\{\mathbf{\Pi}_{LW}\mathbf{W}_5^H\mathbf{\Pi}_{MN}\right\}\left\{\text{vec}\left\{\mathbf{\Pi}_{LW}\mathbf{W}_5^H\mathbf{\Pi}_{MN}\right\}\right\}^H \\
&= \mathbf{\Pi}_{MNLW}\text{vec}\left\{\mathbf{W}_5^H\right\}\left\{\mathbf{\Pi}_{MNLW}\text{vec}\left\{\mathbf{W}_5^H\right\}\right\}^H \\
&= \mathbf{\Pi}_{MNLW}\text{vec}\left\{\mathbf{W}_5^H\right\}\left\{\text{vec}\left\{\mathbf{W}_5^H\right\}\right\}^H\mathbf{\Pi}_{MNLW} \\
&= \mathbf{\Pi}_{LWMN}\mathbf{R}_{nn}^*\mathbf{\Pi}_{LWMN}.
\end{aligned}$$

Similarly, we can prove that:

$$\begin{aligned}
\mathbf{C}_{nn}^{(fba)} &= \mathbb{E}\{\mathbf{n}_{du}\cdot\mathbf{n}_{du}^T\} \\
&= \begin{bmatrix} \mathbf{0} & \mathbf{R}_{nn}\mathbf{\Pi}_{LWMN} \\ \mathbf{\Pi}_{LWMN}\mathbf{R}_{nn}^* & \mathbf{0} \end{bmatrix}.
\end{aligned}$$

□

In the following, we will derive the MSE of the delay estimation using unitary ESPRIT methodology. We first make the following assumptions to facilitate our analysis.

A1: $\mathbf{S}^{(n)H}\mathbf{S}^{(n)}$ is a scaled identity matrix, which leads to the minimized channel estimation error. Moreover, it can be obtained that after the least square channel estimation, we still have the white Gaussian noise.

A2: The sample number LW is large. Note that as long as s_k is known, it is safe to overestimate

L as this will only extend $\mathbf{H}$ by zero columns.

Based on **A1**, we have the following lemma:

Lemma 1. *The covariance matrix* $\mathbf{R}_{nn}$ *and complementary matrix* $\mathbf{C}_{nn}$ *for the delay estimation are given by:*

$$\mathbf{R}_{nn} = \sigma^2 \mathbf{I}_{MN} \otimes \mathbf{G}_g \quad \mathbf{C}_{nn} = \mathbf{0}, \tag{3.9}$$

where $\mathbf{G}_g = diag\left\{\left[|\mathbf{g}_F(-\lceil\frac{LW}{2}\rceil)|^{-2}, \ldots, |\mathbf{g}_F(\lfloor\frac{LW}{2}\rfloor)|^{-2}\right]\right\}$.

Proof. In order to simplify the proof, let $\mathbf{D} = [\text{diag}\{\mathbf{g}_F \mathbf{J}_g\}]^{-1}$. Based on the definition of the covariance matrix, we have

$$\begin{aligned}
\mathbf{R}_{nn} &= \mathbb{E}\left\{\text{vec}\left\{\mathbf{W}_5^T\right\}\text{vec}\left\{\mathbf{W}_5^T\right\}^H\right\} \\
&= \sigma^2\left(\mathbf{I}_{MN} \otimes (\mathbf{J}_g\mathbf{D})^T\right)\left(\mathbf{I}_{MN} \otimes (\mathbf{J}_g\mathbf{D})^*\right) \\
&= \sigma^2 \mathbf{I}_{MN} \otimes \left(\mathbf{D}^T \mathbf{J}_g^T \mathbf{J}_g \mathbf{D}^*\right) \\
&= \sigma^2 \mathbf{I}_{MN} \otimes \mathbf{G}_g.
\end{aligned}$$

We can prove that $\mathbf{C}_{nn} = \mathbf{0}$. □

Similarly, we can also obtain the covariance matrix and complementary matrix for the DoA estimation.

Lemma 2. *The covariance matrix* $\mathbf{R}_{nn}$ *and complementary matrix* $\mathbf{C}_{nn}$ *for the DoA estimation are given by:*

$$\mathbf{R}_{nn} = \sigma^2 \mathbf{G}_g \otimes \mathbf{I}_{MN} \quad \mathbf{C}_{nn} = \mathbf{0}. \tag{3.10}$$

Proof. Based on the definition of the covariance matrix, we have

$$\begin{aligned}
\mathbf{R}_{nn} &= \mathbb{E}\left\{\mathrm{vec}\{\mathbf{W}_5\}\,\mathrm{vec}\{\mathbf{W}_5\}^H\right\} \\
&= \mathbb{E}\left\{\mathrm{vec}\left\{\mathbf{W}_4\mathbf{J}_g\mathbf{D}\right\}\mathrm{vec}\left\{\mathbf{W}_4\mathbf{J}_g\mathbf{D}\right\}^H\right\} \\
&= \mathbb{E}\left\{\left((\mathbf{J}_g\mathbf{D})^T\otimes\mathbf{I}_{MN}\right)\mathrm{vec}\{\mathbf{W}_4\}\,\mathrm{vec}\{\mathbf{W}_4\}^H\left((\mathbf{J}_g\mathbf{D})^*\otimes\mathbf{I}_{MN}\right)\right\} \\
&= \sigma^2\left((\mathbf{J}_g\mathbf{D})^T\otimes\mathbf{I}_{MN}\right)\left((\mathbf{J}_g\mathbf{D})^*\otimes\mathbf{I}_{MN}\right) \\
&= \sigma^2\left(\mathbf{D}^T\mathbf{J}_g^T\mathbf{J}_g\mathbf{D}^*\right)\otimes\mathbf{I}_{MN} \\
&= \sigma^2\mathbf{G}_g\otimes\mathbf{I}_{MN}.
\end{aligned}$$

We can prove that $\mathbf{C}_{nn}=\mathbf{0}$. □

Furthermore, according to **A2**, we have:

Lemma 3. *If the delays of different paths are drawn independently from a continuous distribution, the normalized vectors* $\bar{\mathbf{f}}_k = 1/\sqrt{LW}\mathbf{f}_k, k\in\{1,2,\ldots,P\}$ *are orthogonal, that is,* $1/\sqrt{LW}\mathbf{f}_k \perp$ ***span***$\left\{1/\sqrt{LW}\mathbf{f}_l \mid \forall k\neq\ell\right\}$ *when LW is large and the number of paths is* $P=o(LW)$.

Proof. Let $\mathbf{F}^{-k}=1/\sqrt{LW}\,[\mathbf{f}_1,\ldots,\mathbf{f}_{k-1},\mathbf{f}_{k+1},\ldots,\mathbf{f}_P]$, we have

$$\begin{aligned}
&\lim_{LW\to\infty}\left|\bar{\mathbf{f}}_k^H\mathbf{F}^{-k}\right| \le \lim_{LW\to\infty}\sum_{\ell\neq k}\left|\bar{\mathbf{f}}_k^H\bar{\mathbf{f}}_\ell\right| \\
&= \lim_{LW\to\infty}\sum_{\ell\neq k}\frac{1}{LW}\left|\sum_{n=0}^{LW-1}e^{-j\frac{2\pi}{L}n(\tau_\ell-\tau_k)}\right| \\
&\le \lim_{LW\to\infty}\sum_{\ell\neq k}\frac{1}{LW}\frac{2}{\left|1-e^{-j\frac{2\pi}{L}(\tau_\ell-\tau_k)}\right|} \\
&= 0
\end{aligned}$$

. □

We also have the similar lemma for the normalized steering vector $\bar{\mathbf{a}}_k = 1/\sqrt{MN}\mathbf{a}_k, k=\{1,2,\ldots,P\}$:

Lemma 4. *If the elevation and azimuth angle are both drawn independently from a continuous*

distribution, the normalized array response vector are orthogonal, that is, $\bar{\mathbf{a}}_k \perp \boldsymbol{span}\{\bar{\mathbf{a}}_l \mid \forall k \neq \ell\}$ *when MN is large and the number of paths is* $P = o(MN)$.

Denote $\hat{w}_\ell$ the estimated time delay for the ℓ-th path, the estimation error is given by $\triangle w_\ell = w_\ell - \hat{w}_\ell$. Take the singular value decomposition (SVD) of the noiseless received signal, we have

$$\begin{bmatrix}\mathbf{F}_w^T\mathbf{S} & \mathbf{\Pi}_{LW}\mathbf{F}_w^H\mathbf{S}^*\mathbf{\Pi}_{MN}\end{bmatrix} = \begin{bmatrix}\mathbf{U}_s & \mathbf{U}_n\end{bmatrix}\begin{bmatrix}\mathbf{\Sigma}_s & \mathbf{0}\\ \mathbf{0} & \mathbf{0}\end{bmatrix}\begin{bmatrix}\mathbf{V}_s^H\\ \mathbf{V}_n^H\end{bmatrix} \tag{3.11}$$

It has been derived in [16] that the first order approximation of the mean square error (MSE) for the unitary ESPRIT method is given by:

$$\mathbb{E}\left\{(\triangle w_\ell)^2\right\} = \frac{1}{2}\left(\mathbf{r}_\ell^H \cdot \mathbf{W}_{mat}^* \cdot \mathbf{R}_{nn}^{(fba)T} \cdot \mathbf{W}_{mat}^T \cdot \mathbf{r}_\ell - \mathrm{Re}\left\{\mathbf{r}_\ell^T \cdot \mathbf{W}_{mat} \cdot \mathbf{C}_{nn}^{(fba)} \cdot \mathbf{W}_{mat}^T \cdot \mathbf{r}_\ell\right\}\right). \tag{3.12}$$

The vector $\mathbf{r}_\ell$ and the matrix $\mathbf{W}_{mat}$ are given by

$$\mathbf{r}_\ell = \mathbf{q}_\ell \otimes \left(\left[(\mathbf{J}_1\mathbf{U}_s)^\dagger\left(\mathbf{J}_2/e^{j\cdot w_\ell} - \mathbf{J}_1\right)\right]^T \mathbf{p}_\ell\right) \tag{3.13}$$

$$\mathbf{W}_{mat} = \left(\mathbf{\Sigma}_s^{-1}\mathbf{V}_s^T\right) \otimes \left(\mathbf{U}_n\mathbf{U}_n^H\right), \tag{3.14}$$

where $\mathbf{J}_1 = [\mathbf{I}_{LW-1} \quad \mathbf{0}]$ and $\mathbf{J}_2 = [\mathbf{0} \quad \mathbf{I}_{LW-1}]$ are the selection matrix, $\mathbf{T}$ is the matrix which contains the eigenvector of $(\mathbf{J}_1\mathbf{U}_s)^\dagger(\mathbf{J}_2\mathbf{U}_s)$, $\mathbf{q}_\ell$ is the ℓ-th column of the matrix $\mathbf{T}$, $\mathbf{p}_\ell^T$ is the ℓ-th row of matrix $\mathbf{T}^{-1}$, $\mathbf{R}_{nn}^{(fba)}$ and $\mathbf{C}_{nn}^{(fba)}$ are the covariance matrix and complementary covariance matrix respectively.

It can be seen that (3.12) depends on the singular value decomposition of the noiseless received signal, which is hard to obtain at the base station (BS). In fact, it is extremely difficult to simplify such complicated result in the multiple path case. Fortunately, in the massive MIMO system, it can be significantly simplified in terms of the orthogonality of the steering vector. The simplified result is only related to the real system parameters such as the number of the antennas, number of snapshots and transmit power. Specifically, we have the following theorem:

Theorem 1. *In the massive MIMO system, the MSE of delay estimation using the unitary ESPRIT is given by*

$$\mathbb{E}\left\{(\triangle\tau_\ell)^2\right\} = \frac{L^2\sigma^2}{8\pi^2 MN|\mathbf{b}(\ell)|^2}\frac{|\mathbf{g}_F(-\lceil\frac{LW}{2}\rceil)|^{-2}+|\mathbf{g}_F(\lfloor\frac{LW}{2}\rfloor)|^{-2}}{(LW-1)^2} \tag{3.15}$$

Proof. See Appendix A. □

Remark 1. *In order to facilitate the expression of the underlying MSE, the selected frequency parameter* $\mathbf{g}_F(k)$ *appear in the increasing order from* $-\lceil LW/2\rceil$ *to* $\lfloor LW/2\rfloor$.

Based on proof of **Theorem** 1, we have

Corollary 1.1. *The MSE of the time frequency estimation using the unitary ESPRIT is given by*

$$\mathbb{E}\left\{(\triangle w_\ell)^2\right\} = \frac{\sigma^2}{2MN|\mathbf{b}(\ell)|^2}\frac{|\mathbf{g}_F(-\lceil\frac{LW}{2}\rceil)|^{-2}+|\mathbf{g}_F(\lfloor\frac{LW}{2}\rfloor)|^{-2}}{(LW-1)^2} \tag{3.16}$$

After obtaining the simplified MSE of the delay estimation using unitary ESPRIT, it is straightforward to derive the MSE of w_ℓ using the standard ESPRIT:

Corollary 1.2. *The MSE of the delay estimation using the standard ESPRIT method is the same as that using the unitary ESPRIT method.*

Remark 2. *It can be implied from* (3.15) *that the sample number will have more noticeable effects on the MSE of the delay. We can also easily come to the conclusion that the MSE of the delay is only related to the totally number of antennas, e.g.,* MN.

3.2 Low Complexity Angle Estimation

In this section, we will first introduce a low complexity DoA estimation algorithm based on unitary ESPRIT to jointly estimate the elevation and azimuth angle. The array manifold matrix of an $M \times N$

antenna array can be expressed as:

$$\mathbf{A}(u_\ell, v_\ell) = \mathbf{a}(u_\ell)\mathbf{a}^T(v_\ell),$$

that is, the steering matrix can be decomposed to the product of two steering vectors.

Since we are only interested in DoA estimation, (3.4) can be rewritten as

$$\mathbf{Y}_5 = \mathbf{AS} + \mathbf{W}_5, \tag{3.17}$$

where $\mathbf{S} = \text{diag}\{\mathbf{b}\}\mathbf{F}_w$.

It can be easily verified that $\text{Rank}\{\mathbf{AS}\} = P$ provided that the delay of different paths are distinct. In order to perform the unitary ESPRIT, we also need to use the forward-backward averaging to process the received signal in (3.17).

$$\mathbf{Y}_{au} = [\mathbf{Y}_5 \quad \mathbf{\Pi}_{MN}\mathbf{Y}_5^*\mathbf{\Pi}_{LW}] \tag{3.18}$$

The noiseless received signal can be decomposed into:

$$[\mathbf{AS} \quad \mathbf{\Pi}_{MN}\mathbf{A}^*\mathbf{S}^*\mathbf{\Pi}_{LW}] = \begin{bmatrix}\mathbf{U}_s & \mathbf{U}_n\end{bmatrix}\begin{bmatrix}\mathbf{\Sigma}_s & \mathbf{0} \\ \mathbf{0} & \mathbf{0}\end{bmatrix}\begin{bmatrix}\mathbf{V}_s^H \\ \mathbf{V}_n^H\end{bmatrix}. \tag{3.19}$$

Following our line of work, we have achieved the following relation:

$$\tan(\frac{u_\ell}{2})\mathbf{K}_1\mathbf{a}^R(u_\ell) = \mathbf{K}_2\mathbf{a}^R(u_\ell).$$

Here, $\mathbf{K}_1 = \text{Re}\{\mathbf{Q}_{M-1}^H\mathbf{J}_2\mathbf{Q}_M\}$, $\mathbf{K}_2 = \text{Im}\{\mathbf{Q}_{M-1}^H\mathbf{J}_2\mathbf{Q}_M\}$. $\mathbf{J}_2$ is the $(M-1)\times M$ selection matrix by taking the last $M-1$ rows of $\mathbf{I}_M$, where $\mathbf{I}_M$ is the $M\times M$ identity matrix. $\mathbf{Q}_M$ is the constructed unitary transformation matrix, which changes $\mathbf{a}(u_\ell)$ to the real-valued steering vector $\mathbf{a}^R(u_\ell)$. Ex-

tending the relation to 2D antenna array

$$\tan\left(\frac{u_\ell}{2}\right)\mathbf{K}_1\mathbf{A}^R(u_\ell,v_\ell)=\mathbf{K}_2\mathbf{A}^R(u_\ell,v_\ell). \tag{3.20}$$

where

$$\mathbf{A}^R(u_\ell,v_\ell)=\mathbf{Q}_M^H\mathbf{a}(u_\ell)\mathbf{a}^T(v_\ell)\mathbf{Q}_N^*=\mathbf{a}^R(u_\ell)(\mathbf{a}^R(v_\ell))^T.$$

Furthermore, we can rewrite the formulation in (3.20) as:

$$\tan\left(\frac{u_\ell}{2}\right)\mathbf{K}_{x1}\mathrm{vec}\left\{\mathbf{A}^R(u_\ell,v_\ell)\right\}=\mathbf{K}_{x2}\mathrm{vec}\left\{\mathbf{A}^R(u_\ell,v_\ell)\right\}$$

where $\mathbf{K}_{x1}\triangleq\mathbf{I}_N\otimes\mathbf{K}_1$, and $\mathbf{K}_{x2}\triangleq\mathbf{I}_N\otimes\mathbf{K}_2$. Accordingly, we can specify an $MN\times P$ real-valued array manifold matrix:

$$\mathbf{A}^R\triangleq\left[\begin{array}{ccc}\mathrm{vec}\left\{\mathbf{a}^R(u_1,v_1)\right\} & \ldots & \mathrm{vec}\left\{\mathbf{a}^R(u_P,v_P)\right\}\end{array}\right]$$

Then, we have the shift-invariance equation:

$$\mathbf{K}_{x1}\mathbf{A}^R\mathbf{\Omega}_x=\mathbf{K}_{x2}\mathbf{A}^R \tag{3.21}$$

where

$$\mathbf{\Omega}_x\triangleq\mathrm{diag}\left\{\tan\left(\frac{u_1}{2}\right),\tan\left(\frac{u_2}{2}\right),\ldots,\tan\left(\frac{u_P}{2}\right)\right\}.$$

It is important to note that after the unitary transformation, all the matrices become real-valued matrices. This will significantly reduce the computational complexity.

Similarly, for $\mathbf{a}(v_\ell)$, we can conduct the same process. Let $\mathbf{K}_3=\mathrm{Re}\left\{\mathbf{Q}_{N-1}^H\mathbf{J}_2'\mathbf{Q}_N\right\}$, and $\mathbf{K}_4=\mathrm{Im}\left\{\mathbf{Q}_{N-1}^H\mathbf{J}_2'\mathbf{Q}_N\right\}$, where $\mathbf{J}_2'$ is the $(N-1)\times N$ matrix constructed by taking the last $(N-1)$ rows of $\mathbf{I}_N$. Accordingly, we have

$$\mathbf{K}_{y1}\mathbf{A}^R\mathbf{\Omega}_y=\mathbf{K}_{y2}\mathbf{A}^R \tag{3.22}$$

where $\mathbf{K}_{y1} \triangleq \mathbf{K}_3 \otimes \mathbf{I}_M$, $\mathbf{K}_{y2} \triangleq \mathbf{K}_4 \otimes \mathbf{I}_M$, and

$$\mathbf{\Omega}_y \triangleq \text{diag}\left\{\tan\left(\frac{v_1}{2}\right), \tan\left(\frac{v_2}{2}\right), \ldots, \tan\left(\frac{v_P}{2}\right)\right\}$$

Let $\mathbf{U}_s$ be the signal subspace and $\mathbf{T}$ be the nonsingular transformation matrix, we have $\mathbf{U}_s = \mathbf{A}^R\mathbf{T}$ since the array steering matrix $\mathbf{A}^R$ and the matrix $\mathbf{U}_s$ span the same column space in the absence of noise or with an infinite number of measurements. Under the noisy case or with a finite number of measurements, this expression holds approximately. Substitute this relation into (3.21), we have

$$\mathbf{K}_{x1}\mathbf{U}_s\Lambda_x = \mathbf{K}_{x2}\mathbf{U}_s \tag{3.23}$$

where $\mathbf{\Lambda}_x \triangleq \mathbf{T}^{-1}\mathbf{\Omega}_x\mathbf{T}$. Similarly, we also have

$$\mathbf{K}_{y1}\mathbf{U}_s\Lambda_y = \mathbf{K}_{y2}\mathbf{U}_s \tag{3.24}$$

where $\mathbf{\Lambda}_y \triangleq \mathbf{T}^{-1}\mathbf{\Omega}_y\mathbf{T}$. From (3.23) and (3.24), we can solve for $\hat{\mathbf{\Lambda}}_x$ and $\hat{\mathbf{\Lambda}}_y$ based on the estimated signal subspace using least square type of methods. Let the eigenvalues of the $P \times P$ complex matrix $\hat{\mathbf{\Lambda}}_x + j\hat{\mathbf{\Lambda}}_y$ be $\hat{\lambda}_\ell, \ell = 1, 2, \ldots, P$. u_ℓ and v_ℓ can be estimated from:

$$\hat{u}_\ell = 2\tan^{-1}\left\{\text{Re}\left(\hat{\lambda}_\ell\right)\right\} \quad \hat{v}_\ell = 2\tan^{-1}\left\{\text{Im}\left(\hat{\lambda}_\ell\right)\right\}$$

Accordingly, the DoAs of interest are obtained through simple parameter transformation.

In the massive MIMO system, we have the following theorem.

Theorem 2. *For the case of 3D DoA estimation based on a uniform planar array of $M \times N$ ele-*

ments, the mean square errors of the elevation and azimuth angle estimation are given by:

$$\mathbb{E}\left\{(\triangle\theta_\ell)^2\right\} = \frac{\sigma^2}{\pi^2\sin^2(\theta_\ell)}\frac{\sum_{i=-\lceil\frac{LW}{2}\rceil}^{\lfloor\frac{LW}{2}\rfloor}|\mathbf{g}_F(i)|^{-2}}{|\mathbf{b}(\ell)|^2(LW)^2(M-1)^2N}$$
$$\mathbb{E}\left\{(\triangle\phi_\ell)^2\right\} = \frac{\sigma^2}{\pi^2\sin^2(\theta_\ell)}\frac{\sum_{i=-\lceil\frac{LW}{2}\rceil}^{\lfloor\frac{LW}{2}\rfloor}|\mathbf{g}_F(i)|^{-2}}{|\mathbf{b}(\ell)|^2(LW)^2}\left(\frac{\cot^2(\theta_\ell)\cot^2(\phi_\ell)}{(M-1)^2N}+\frac{1}{\sin^2(\phi_\ell)(N-1)^2M}\right). \tag{3.25}$$

.

Proof. See Appendix B. □

Based on the proof of **Theorem** 2, it is straightforward to obtain the MSE of the spatial frequencies u_ℓ and v_ℓ as follows:

Corollary 2.1. *In the massive MIMO system, the MSE of the spatial frequencies u_ℓ, v_ℓ using the unitary ESPRIT are given by:*

$$\mathbb{E}\left\{(\triangle u_\ell)^2\right\} = \frac{\sigma^2}{|\mathbf{b}(\ell)|^2(LW)^2}\frac{\sum_{i=-\lceil\frac{LW}{2}\rceil}^{\lfloor\frac{LW}{2}\rfloor}|\mathbf{g}_F(i)|^{-2}}{(M-1)^2N}$$
$$\mathbb{E}\left\{(\triangle v_\ell)^2\right\} = \frac{\sigma^2}{|\mathbf{b}(\ell)|^2(LW)^2}\frac{\sum_{i=-\lceil\frac{LW}{2}\rceil}^{\lfloor\frac{LW}{2}\rfloor}|\mathbf{g}_F(i)|^{-2}}{(N-1)^2M} \tag{3.26}$$

.

For the 2D standard ESPRIT method, following the similar proof procedure of **Theorem** 2, we have the following corollary.

Corollary 2.2. *In the massive MIMO system, the MSE of elevation and azimuth estimation using the 2D standard ESPRIT is the same as that using the 2D unitary ESPRIT.*

It is clear that the angles and delay can be estimated independently of each other, by directly working on the rows and columns of the transformed channel matrix. However, this does not give a pairing between angles and the corresponding delay. We will introduce the joint angle and delay

estimation algorithm for rectangular planar array and derive the corresponding MSE in the massive MIMO system in the following chapter.

Chapter 4

Joint Angle and Delay Estimation

In this chapter, we will construct a space-time manifold through vectorization and jointly estimate the delay and DoAs using ESPRIT algorithm in Chapter 4.1. The MSE of the joint angle and delay estimation using ESPRIT method is derived in Chapter 4.2.

4.1 Matrix-based Joint Estimation Using ESPRIT Method

Recall that our received signal after deconvoluation of $g(t)$ is given in (3.4):

$$\mathbf{Y}_5 = \mathbf{A}\text{diag}\{\mathbf{b}\}\mathbf{F}_w + \mathbf{W}_5.$$

In order to estimate angle and delay jointly, the first step is to construct the channel matrix which involves delay, elevation angle and azimuth angle, which can be obtained either through stacking the received signal $\mathbf{Y}_5$ into Hankel matrix or taking vectorization. In the next two sections, we will give a detailed description of the two methods and propose our own matrix transformation methodology.

4.1.1 Matrix Transformation through Hankel Matrix

The main idea now is as follows. From $\mathbf{Y}_5$, we can construct a Hankel matrix $\mathbf{Y}_H$ by left-shifting and stacking m copies of $\mathbf{Y}_5$. For $1 \leq i \leq m$, define the left-shifted matrix $\hat{\mathbf{Y}}_H^{(i)} := \mathbf{Y}_5\,(:, i : LW - m + i)$. Note that the notation $(:, i : LW - m + 1)$ indicates taking columns i through $LW - m + 1$ of a matrix. Then the Hankel matrix $\mathbf{Y}_H$ can be defined as

$$\mathbf{Y}_H = \begin{bmatrix} \hat{\mathbf{Y}}_H^{(i)} \\ \vdots \\ \hat{\mathbf{Y}}_H^{(m)} \end{bmatrix} \tag{4.1}$$

where $\mathbf{Y}_H \in \mathbb{C}^{mMN \times LW - m + 1}$.

The motivation behind such matrix stacking is that $\mathbf{Y}_H$ has a factorization as [18]:

$$\begin{aligned} \mathbf{Y}_H &= \mathbf{A}_H \mathrm{diag}\{\mathbf{b}\}\,\mathbf{F}_w, \\ \mathbf{A}_H &= \mathbf{A} \diamond \begin{bmatrix} 1 & \dots & 1 \\ e^{-j(2\pi/L)\tau_1} & \dots & e^{-j(2\pi/L)\tau_P} \\ \vdots & & \vdots \\ e^{-j(m-1)(2\pi/L)\tau_1} & \dots & e^{-j(m-1)(2\pi/L)\tau_P} \end{bmatrix} \end{aligned} \tag{4.2}$$

where $\diamond$ denotes the Khatri-Rao product, i.e., a column-wise Kronecker product. If we choose the stacking parameters, m, to make the Hankel matrix $\mathbf{Y}_H$ satisfy the following condition:

$$MNm \geq P,$$

$$LW - m + 1 \geq P,$$

then we can estimate $\mathbf{A}_H$ up to an $P \times P$ factor at the right as long as all factors are full rank. Hence we can estimate the unknowns through shift invariance property.

Nevertheless, the drawback of stacking the received signal $\mathbf{Y}_5$ into a Hankel matrix is that the degree of freedom that we can utilize to perform the ESPRIT method is diminished. To be

specific, the number of rows in our Hankel matrix is mMN, which means the whole degree of freedom, $LWMN$, has not been fully exploited. In order to combat this disadvantage, in the next section, matrix vectorization is used to transform the received matrix into a space-time manifold matrix which involves both delay and angle estimation.

4.1.2 Matrix Transformation through Vectorization

The matrix vectorization and Khatri-Rao has the following relationship [23]:

$$\mathrm{vec}\left(\mathbf{AXB}\right) = \left(\mathbf{B}^T \diamond \mathbf{A}\right) \mathrm{vecd}\left(\mathbf{X}\right), \tag{4.3}$$

where $\mathbf{A}, \mathbf{B}, \mathbf{X}$ denote the arbitrary matrix which dimension meet the requirement of the matrix multiplicity, $\mathrm{vecd}\left(\right)$ indicates the vectorization operator which selects only the diagonal elements of the matrix into a vector.

In terms of (4.3), we can take vectorization of the received signal:

$$\mathbf{y}_v^{(n)} = \mathbf{A}(\tau, \theta, \phi)\mathbf{b}(n) + \mathrm{vec}\left\{\mathbf{W}_5^{(n)}\right\}. \tag{4.4}$$

Collect $\mathbf{y}_v^{(n)}$ during K time intervals, we have

$$\mathbf{Y}_v = \mathbf{A}(\tau, \theta, \phi)\mathbf{B} + \mathbf{W}_6, \tag{4.5}$$

where

$$\begin{aligned}
\mathbf{B} &= \begin{bmatrix} \mathbf{b}(1) & \mathbf{b}(2) & \dots & \mathbf{b}(K) \end{bmatrix} \\
\mathbf{W}_6 &= \begin{bmatrix} \mathrm{vec}\left\{\mathbf{W}_5^{(1)}\right\} & \mathrm{vec}\left\{\mathbf{W}_5^{(2)}\right\} & \dots & \mathrm{vec}\left\{\mathbf{W}_5^{(K)}\right\} \end{bmatrix} \\
\mathbf{A}(\tau, \theta, \phi) &= \mathbf{F}_w^T \diamond \mathbf{A}
\end{aligned}$$

Since $\mathbf{F}_w$ and $\mathbf{A}$ are the time delay matrix and array matrix respectively with Vandermonde

structure. Hence we can utilize the shift-invariance property of this highly structured matrix to jointly estimate the unknowns based on ESPRIT-type algorithms.

To estimate w_ℓ, we should take the first and respectively last $MN(LW-1)$ rows of channel matrix as two submatrices, while for θ_ℓ estimation, we may take its first and respectively last $M-1$ rows for all LWN blocks of channel matrix, similarly, for ϕ_ℓ estimation, we may take its first and respectively last $N-1$ rows for all LWM blocks. Hence, we may define the selection matrices as follows:

$$\begin{aligned}
&\mathbf{J}_1^{(1)} = [\mathbf{I}_{LW-1}\ \mathbf{0}] \otimes \mathbf{I}_{MN} \quad \mathbf{J}_2^{(1)} = [\mathbf{0}\ \mathbf{I}_{LW-1}] \otimes \mathbf{I}_{MN} \\
&\mathbf{J}_1^{(2)} = \mathbf{I}_{LWN} \otimes [\mathbf{I}_{M-1}\ \mathbf{0}] \quad \mathbf{J}_2^{(2)} = \mathbf{I}_{LWN} \otimes [\mathbf{0}\ \mathbf{I}_{M-1}] \\
&\mathbf{J}_1^{(3)} = \mathbf{I}_{LW} \otimes [\mathbf{I}_{N-1}\ \mathbf{0}] \otimes \mathbf{I}_M \quad \mathbf{J}_2^{(3)} = \mathbf{I}_{LW} \otimes [\mathbf{0}\ \mathbf{I}_{N-1}] \otimes I_M
\end{aligned}$$

Through shift-invariance property, we can write:

$$\begin{aligned}
\mathbf{J}_1^{(1)}\mathbf{A}(\tau,\theta,\phi)\mathbf{W} &= \mathbf{J}_2^{(1)}\mathbf{A}(\tau,\theta,\phi) \\
\mathbf{J}_1^{(2)}\mathbf{A}(\tau,\theta,\phi)\Theta &= \mathbf{J}_2^{(2)}\mathbf{A}(\tau,\theta,\phi) \\
\mathbf{J}_1^{(3)}\mathbf{A}(\tau,\theta,\phi)\Phi &= \mathbf{J}_2^{(3)}\mathbf{A}(\tau,\theta,\phi),
\end{aligned} \tag{4.6}$$

where $\mathbf{W}$, Θ and Φ are the corresponding diagonal matrices, containing desired parameters for each path.

Then we can directly apply the ESPRIT-type algorithm to jointly estimate the delay and DoAs. Note that, the advantage of JADE is that it can work even when the number of paths exceeds the number of antennas ($P > MN$). We only need the space-time manifold matrix to be a tall matrix, which means $P < MNLW$. The unitary ESPRIT can also be performed through the forward-backward averaging which can provide the correctly pairing between the delay and the corresponding DoAs through Jacobian matrix [17].

4.2 Mean Square Error (MSE) of Matrix-Based ESPRIT Method

In this section, we will focus on the theoretical analysis of the mean square error (MSE) of the matrix-based ESPRIT method. For simplicity, we denote $\mu_\ell^{(1)} = u_\ell$, $\mu_\ell^{(2)} = v_\ell$ and $\mu_\ell^{(3)} = w_\ell$. Define the estimation error $\triangle\mu_\ell^{(r)} = \hat{\mu}_\ell^{(r)} - \mu_\ell^{(r)}$, where $\hat{\mu}_\ell^{(r)}$ is the estimated result.

The noiseless signal in (4.5) can be decomposed into:

$$\mathbf{A}(\tau,\theta,\phi)\mathbf{B} = \begin{bmatrix} \mathbf{U}_s & \mathbf{U}_n \end{bmatrix} \begin{bmatrix} \mathbf{\Sigma}_s & \mathbf{0} \\ \mathbf{0} & \mathbf{0} \end{bmatrix} \begin{bmatrix} \mathbf{V}_s^H \\ \mathbf{V}_n^H \end{bmatrix} \tag{4.7}$$

The first order approximation of the mean square error (MSE) for the ℓ-th spatial frequency in the r-th mode is given by [16]

$$\begin{aligned} \mathbb{E}\left\{ \left(\triangle\mu_\ell^{(r)} \right)^2 \right\} = \frac{1}{2} \Big(& \mathbf{r}_\ell^{(r)H} \cdot \mathbf{W}_{mat}^{*} \cdot \mathbf{R}_{nn}^{(fba)T} \cdot \mathbf{W}_{mat}^{T} \cdot \mathbf{r}_\ell^{(r)} \\ -\mathrm{Re}\left\{ \mathbf{r}_\ell^{(r)T} \cdot \mathbf{W}_{mat} \cdot \mathbf{C}_{nn}^{(fba)} \cdot \mathbf{W}_{mat}^{T} \cdot \mathbf{r}_\ell^{(r)} \right\} \Big), & r \in \{1,2,3\}. \end{aligned} \tag{4.8}$$

The vector $\mathbf{r}_\ell^{(r)}$ and the matrix $\mathbf{W}_{mat}$ are given by

$$\mathbf{r}_\ell^{(r)} = \mathbf{q}_\ell \otimes \left(\left[\left(\mathbf{J}_1^{(r)} \mathbf{U}_s \right)^\dagger \left(\mathbf{J}_2^{(r)} / e^{j\cdot\mu_\ell^{(r)}} - \mathbf{J}_1^{(r)} \right) \right]^T \mathbf{p}_\ell \right) \tag{4.9}$$

$$\mathbf{W}_{mat} = \left(\mathbf{\Sigma}_s^{-1} \mathbf{V}_s^T \right) \otimes \left(\mathbf{U}_n \mathbf{U}_n^H \right), \tag{4.10}$$

where $\mathbf{q}_\ell$ is the ℓ-th column of the transformation matrix $\mathbf{T}$, $\mathbf{p}_\ell$ is the ℓ-th row of matrix $\mathbf{T}^{-1}$, $\mathbf{R}_{nn}^{(fba)}$ and $\mathbf{C}_{nn}^{(fba)}$ are the covariance and complementary covariance matrix respectively.

Lemma 5. *The MSE of the JADE using unitary ESPRIT is given by* (4.8) *in which the covariance*

and complementary covariance matrix are as follows:

$$\begin{aligned}\mathbf{R}_{nn}^{(fba)} &= \begin{bmatrix} \mathbf{R}_{nn} & \mathbf{0} \\ \mathbf{0} & \mathbf{\Pi}_{LWMN}\mathbf{R}_{nn}^{*}\mathbf{\Pi}_{LWMN} \end{bmatrix} \\ \mathbf{C}_{nn}^{(fba)} &= \begin{bmatrix} \mathbf{0} & \mathbf{R}_{nn}\mathbf{\Pi}_{LWMN} \\ \mathbf{\Pi}_{LWMN}\mathbf{R}_{nn}^{*} & \mathbf{0}, \end{bmatrix}\end{aligned} \tag{4.11}$$

where $\mathbf{R}_{nn} = \sigma^2\mathbf{I}_K \otimes \mathbf{G}_g \otimes \mathbf{I}_{MN}$.

Proof. We only need to investigate the covariance matrix of the received signal:

$$\begin{aligned}\mathbf{R}_{nn} &= \operatorname{vec}\{\mathbf{W}_6\}\{\operatorname{vec}\{\mathbf{W}_6\}\}^H \\ &= \begin{bmatrix} \operatorname{vec}\left\{\mathbf{W}_5^{(1)}\right\} \\ \vdots \\ \operatorname{vec}\left\{\mathbf{W}_5^{(K)}\right\} \end{bmatrix} \begin{bmatrix} \left\{\operatorname{vec}\left\{\mathbf{W}_5^{(1)}\right\}\right\}^H & \dots & \left\{\operatorname{vec}\left\{\mathbf{W}_5^{(K)}\right\}\right\}^H \end{bmatrix} \\ &= \begin{bmatrix} \sigma^2\mathbf{G}_g \otimes \mathbf{I}_{MN} & \dots & 0 \\ \vdots & \ddots & \vdots \\ 0 & \dots & \sigma^2\mathbf{G}_g \otimes \mathbf{I}_{MN} \end{bmatrix} \\ &= \sigma^2\mathbf{I}_K \otimes \mathbf{G}_g \otimes \mathbf{I}_{MN}.\end{aligned} \tag{4.12}$$

Substitute (4.12) into (4.8), the prove is finished. □

For the standard ESPRIT, we have the simplified MSE of the elevation angle θ_ℓ and azimuth angle ϕ_ℓ in the massive MIMO system as follows:

Theorem 3. *In the case of 3D DoA estimation based on a uniform planar array of* $M \times N$ *elements,*

the mean square errors of the elevation and azimuth angle estimation are given by:

$$\mathbb{E}\left\{(\triangle\theta_\ell)^2\right\} = \frac{\sigma^2}{\pi^2\sin^2(\theta_\ell)}\frac{\mathbf{R}_{ss}^{-1}(\ell,\ell)\left(|\mathbf{g}_F(-\lceil\frac{LW}{2}\rceil)|^{-2}+|\mathbf{g}_F(\lfloor\frac{LW}{2}\rfloor)|^{-2}\right)}{2K(M-1)^2NLW}$$
$$\mathbb{E}\left\{(\triangle\phi_\ell)^2\right\} = \frac{\sigma^2}{\pi^2\sin^2(\theta_\ell)}\frac{\mathbf{R}_{ss}^{-1}(\ell,\ell)\left(|\mathbf{g}_F(-\lceil\frac{LW}{2}\rceil)|^{-2}+|\mathbf{g}_F(\lfloor\frac{LW}{2}\rfloor)|^{-2}\right)}{2KLW}\left(\frac{\cot^2(\theta_\ell)\cot^2(\phi_\ell)}{(M-1)^2N}\right.$$
$$\left.+\frac{1}{\sin^2(\phi_\ell)(N-1)^2M}\right) \tag{4.13}$$

Proof. See Appendix C. □

Based on the proof of **Theorem** 3, we can obtain the MSE of the delay as follows:

Corollary 3.1. *The MSE of the delay estimation using the standard ESPRIT is given by:*

$$\mathbb{E}\left\{(\triangle\tau_\ell)^2\right\} = \frac{L^2}{4\pi^2}\frac{\sigma^2\mathbf{R}_{ss}^{-1}(\ell,\ell)\left(|\mathbf{g}_F(-\lceil\frac{LW}{2}\rceil)|^{-2}+|\mathbf{g}_F(\lfloor\frac{LW}{2}\rfloor)|^{-2}\right)}{2K(LW-1)^2MN} \tag{4.14}$$

4.3 Cramer-Rao Bound

The CRB provides a lower bound on the variance of any unbiased estimator. The CRB depends on whether the path fading are modeled as unknown deterministic quantities or as random variables with a know distribution. In the case of the deterministic fading scenario in which the noise is assumed to be random and the fading is assumed to be unknown constant, if we apply the vectorization operator to the noise-perturbed model in (2.7), we can obtain

$$\mathbf{h} := \mathbf{U}\mathbf{b} + \mathbf{v} \tag{4.15}$$

where $\mathbf{U} = \mathbf{G}^T \diamond \mathbf{A}$, $\mathbf{b} = [b(1),\ldots,b(P)]^T$ and $\mathbf{v}$ is the noise on the channel estimation.

Then CRB for DoA with delay spread was derived in [24], which is given by

$$\mathrm{CRB}(\boldsymbol{\alpha},\boldsymbol{\tau}) = \frac{\sigma^2}{2K}\mathrm{Real}\left\{\mathfrak{B}^H\mathbf{D}^H\mathbf{P}_U\mathbf{D}\mathfrak{B}\right\}^{-1} \tag{4.16}$$

where $\boldsymbol{\alpha} = [\theta_1,\ldots,\theta_P,\phi_1,\ldots,\phi_P]^T$, $\boldsymbol{\tau} = [\tau_1,\ldots,\tau_P]^T$, $\mathfrak{B} = \mathbf{I}_2 \otimes \mathrm{diag}\{\mathbf{b}(n)\}$, $\mathbf{P}_U = \mathbf{I} - \mathbf{U}\left(\mathbf{U}^*\mathbf{U}\right)^{-1}\mathbf{U}^*$, and $\mathbf{D} = \mathbf{U}'$. Here prime denotes differential.

For a Rayleigh-fading channel, the path fadings have a zero-mean complex Gaussian distribution, with some covariance matrix $\mathbf{R}_b$. The CRB in this case is also given in [24]:

$$\mathrm{CRB}(\boldsymbol{\alpha},\boldsymbol{\tau}) = \frac{\sigma^2}{2K}\mathrm{Real}\left\{\mathbf{D}^*\mathbf{P}_U\mathbf{D} \odot \left(\mathbf{1}_{3\times 3} \otimes \mathbf{R}_b\mathbf{U}^H\mathbf{R}_h^{-1}\mathbf{U}\mathbf{R}_b\right)^T\right\}^{-1} \tag{4.17}$$

where $\mathbf{R}_h = \mathbf{U}\mathbf{R}_b\mathbf{U}^H + \sigma^2/K\mathbf{I}$.

Chapter 5

Performance Evaluation

In this chapter, we will evaluate the performance of the matrix-based ESPRIT method. First, we can directly follow the one dimensional unitary ESPRIT algorithm to obtain the delay estimation. Assume that there are five resolvable paths, which is the typical number in the outdoor millimeter wave system [19]. The known pulse shape function we use is a raised cosine signal, with roll-off factor 0.5 and oversampling rate 2 compared to the normalized symbol rate. The received signal noise ratio (SNR) is defined as SNR $= \mathbb{E}\{s\} \sum_{i=1}^{P} \alpha_i^2 / \sigma^2$. The performance of delay under different SNR, ranging form -4 dB to 24 dB (dynamic range of SNR in a cellular environment), is shown in Fig. 5.1. We can see from the figure that our analytic result matches the empirical results.

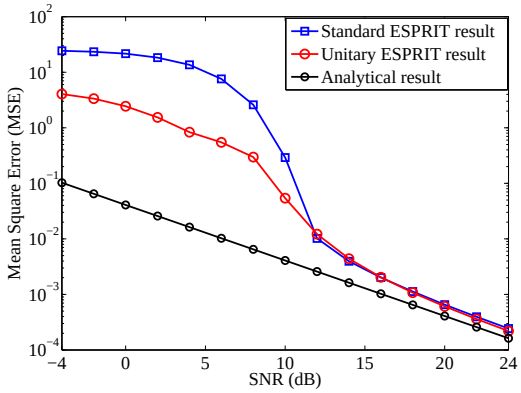

Figure 5.1: MSE of separated delay estimation

The MSE of the spatial frequency v_ℓ using unitary ESPRIT method is illustrated in Fig. 5.2. It

can be seen that the MSE of the spatial frequency v_ℓ decreases with the increasing of the number of antennas horizontally. Moreover, as the SNR increases, the empirical result approaches the analytical one asymptotically, which verifies our analytical result. We can also obtain the same result for spatial frequency u_ℓ, which is shown in . The performance of angle estimation based

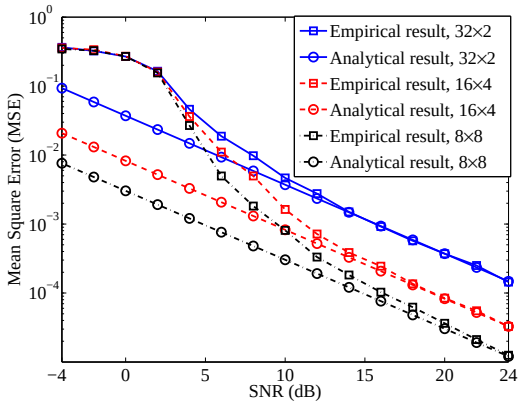

Figure 5.2: MSE of separated spatial frequency v_ℓ

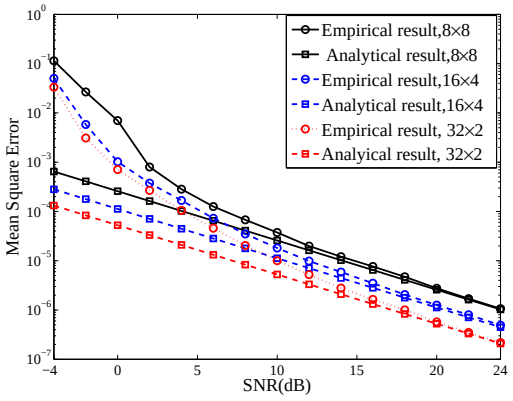

Figure 5.3: MSE of separated spatial frequency u_ℓ

on unitary ESPRIT is evaluated in Fig. 5.4 and Fig. 5.5 under various antenna configurations. The elevation angle is restricted to the range $[11^\circ, 82^\circ]$ while the azimuth angle is within $[10^\circ, 80^\circ]$. It can be seen from Fig. 5.4 that the MSE of the elevation angle estimation with different antenna structures are almost parallel to each other in the high SNR regime. Furthermore, it is interesting to note that the MSE of azimuth angle estimation doesn't scale proportionally to the number of antennas horizontally, as shown in Fig. 5.5. We observe that the MSE of azimuth estimation of a

4×16 array is even larger than that of 8×8, which seems a little bit counter-intuitive. The reason for this phenomenon to happen is because azimuth estimation is actually coupled with elevation estimation. In the case of 8×8 antenna configuration, the performance of elevation is so poor that it affects the performance of azimuth estimation.

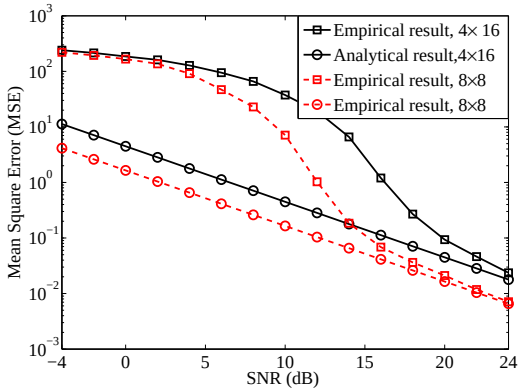

Figure 5.4: MSE of separated elevation angle estimation

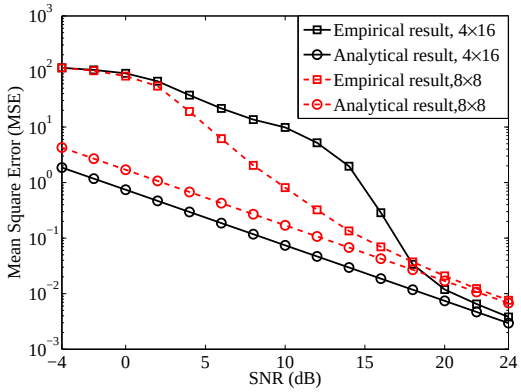

Figure 5.5: MSE of separated azimuth angle estimation

The MSE of the delay estimation using the joint angle and delay estimation (JADE) methodology is shown in Fig. 5.6. In contrast with the separated method, the performance of the standard ESPRIT is proportional to the number of the intervals, which is equivalent to the “training sequence". The length of the “training sequence" K also impacts the MSE of the delay and angle estimation. Here K is set to be 15. It can be clearly seen from Fig. 5.6 that the proposed JADE method can achieve a better performance compared to the separated method. Moreover, we can

observed that in the high SNR regime, the empirical MSE of the JADE method matches our analytical result proposed in **Corollary** 3.1. The similar results can be obtained for the MSE of the angle estimation. The Cramer-Rao bound(CRB) of the joint angle and delay estimation (JADE) methodology can be seen in Fig. 5.7

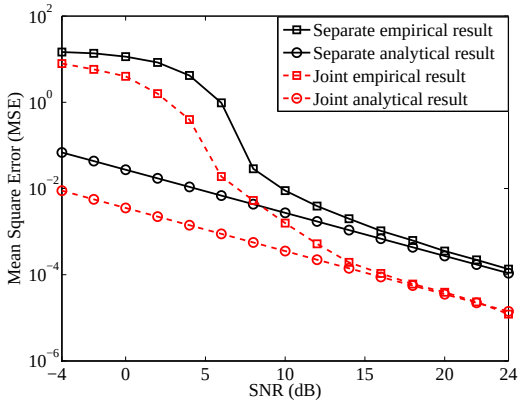

Figure 5.6: MSE of joint and separated delay estimation

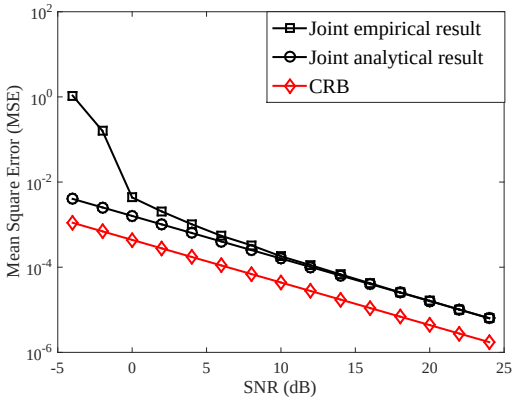

Figure 5.7: The CRB of delay estimation

Chapter 6

Conclusion and Future Work

Joint and separated angle and delay estimation methodologies in 3D massive MIMO millimeter wave systems are investigated in the thesis. Specifically, the mean square error (MSE) of the ESPRIT method are analyzed and the simplified results are obtained.

First, we investigate the separate angle and delay estimation method using standard and unitary ESPRIT. In light of the orthogonality of the steering vector in the massive MIMO system, we obtain the simplified MSE of the ESPRIT-type method. Secondly, we derive the simplified expression of the MSE in the massive MIMO system. The performance of the elevation and azimuth angle under various antenna configurations is investigated.

For the 3D channel sounding, we can observe that the azimuth angle estimation actually depends heavily on the elevation angle estimation, and its performance is more vulnerable. Using ESPRIT-type DoA algorithms, a 8×8 array may outperform a 4×16 array in both elevation and azimuth angle estimation. This is of significant meaning to 3D antenna array design for the future "massive MIMO" research. For example, this result may shed light on the actual antenna configuration as well as the reference signal (pilot) design for 5G massive MIMO base stations/systems.

There are still many open issues related to DoA estimation we can investigated in the future:

- Full-dimension multi-input-multi-output (FD-MIMO) and user-equipment (UE) specific elevation beamforming were identified as one promising technology to further increase spectral

efficiency. FD-MIMO places a large number of active antenna elements in a two-dimensional grid at the base station, which can support elevation and azimuth beamforming. In October 2014, a new study item on FD-MIMO and UE-specific elevation beamforming was initiated in the 3GPP [25]. Samsung, which is now leading the standard and implementation of FD-MIMO, has already implemented 2D active antenna array for FD-MIMO system [26]. In order to perform the two-dimensional beamforming at the base station, it is crucial to perform the two-dimensional DoA estimation to estimate both the elevation and azimuth angle. How to make the accurate DoA estimation with the low complexity in FD-MIMO system will still be a challenge [27].

- Although theoretically the system performance in both energy saving and spectrum efficiency can be increase dramatically in massive MIMO system. However, in practice, the performance will be affected by the acquisition of the channel state information (CSI) [28]. In TDD system, the uplink pilot in one cell may be contaminated by the same pilot from other cells, which will diminish the performance gain in the downlink beamforming. Even though there are already some literature dealing with the pilot contamination via DoA estimation [29], there are still many open problems in this topic.

- In the massive MIMO system, due to the orthogonality property, the DoA steering vector can be used to perform the downlink beamforming [30]. In our previous paper [31], the impact of DoA estimation error on the underlying achievable rate is analyzed in single-user single-cell MIMO system. How to extend to multi-user, multi-cell MIMO scenario is still an open question.

References

[1] ITU-D, *World Telecommunication/ICT Indicators Database 2013*. International Telecommunications Union (ITU), June 2013.

[2] Cisco Systems, *Cisco Visual Networking Index: Forecast and Methodology, 2012-2017*. Cisco, May 2013.

[3] ——, *Cisco Visual Networking Index: Global Mobile Data Traffic Forecast Update, 2012-2017*. Cisco, May 2013.

[4] L. Liu, R. Chen, S. Geirhofer, K. Sayana, Z. Shi, and Y. Zhou, "Downlink MIMO in LTE-Advanced: SU-MIMO vs. MU-MIMO," *IEEE Communications Magazine*, vol. 50, no. 2, pp. 140–147, February 2012.

[5] T. L. Marzetta, "Noncooperative cellular wireless with unlimited numbers of base station antennas," *IEEE Transactions on Wireless Communications*, vol. 9, no. 11, pp. 3590–3600, November 2010.

[6] H. Huh, G. Caire, H. C. Papadopoulos, and S. A. Ramprashad, "Achieving "Massive MIMO" spectral efficiency with a not-so-large number of antennas," *IEEE Transactions on Wireless Communications*, vol. 11, pp. 3226–3239, September 2012.

[7] B. Ng, Y. Kim, J. Lee, Y. Li, Y. Nam, J. Zhang, and K. Sayana, "Fulfilling the promise of massive mimo with 2d active antenna array," in *IEEE GLOBECOM Workshop on Emerging Technologies for LTE-Advanced and Beyond-4G*, December 2012.

[8] Y.-H. Nam, B. L. Ng, K. Sayana, Y. Li, J. Zhang, Y. Kim, and J. Lee, "Full-dimension mimo (fd-mimo) for next generation cellular technology," *IEEE Communications Magazine*, vol. 51, no. 6, pp. 172–179, June 2013.

[9] B. Yang, K. Letaief, R. S. Cheng, and Z. Cao, "Channel estimation for ofdm transmission in multipath fading channels based on parametric channel modeling," *IEEE Transactions on Communications*, vol. 49, no. 3, pp. 467–479, March 2001.

[10] M. Larsen, A. Swindlehurst, and T. Svantesson, "Performance Bounds for MIMO-OFDM Channel Estimation," *IEEE Transactions on Signal Processing*, vol. 57, no. 5, pp. 1901–1916, May 2009.

[11] M. Wax and A. Leshem, "Joint estimation of time delays and directions of arrival of multiple reflections of a known signal," *IEEE Transactions on Signal Processing*, vol. 45, no. 10, pp. 2477–2484, October 1997.

[12] A. L. Swindlehurst, "Time-delay and spatial signature estimation using known asynchronous signals," *IEEE Transactions on Signal Processing*, vol. 46, no. 2, pp. 449–461, Feburary 1998.

[13] Y.-Y. Wang, J.-T. Chen, and W.-H. Fang, "TST-MUSIC for joint DOA-delay estimation," *IEEE Transactions on Signal Processing*, vol. 49, no. 4, pp. 721–729, April 2001.

[14] R. Roy and T. Kailath, "Esprit-estimation of signal parameters via rotational invariance techniques," *IEEE Transactions on Acoustics, Speech and Signal Processing*, vol. 37, no. 7, pp. 984–995, 1989.

[15] F. Li, H. Liu, and R. J. Vaccaro, "Performance analysis for DOA estimation algorithms: unification, simplification, and observations," *IEEE Transactions on Aerospace and Electronic Systems*, vol. 29, no. 4, pp. 1170–1184, October 1993.

[16] F. Roemer, M. Haardt, and G. Del Galdo, "Analytical performance assessment of multi-dimensional matrix-and tensor-based esprit-type algorithms," *IEEE Transactions on Signal Processing*, vol. 62, no. 10, pp. 2611–2625, May 2014.

[17] M. Haardt and J. A. Nossek, "Simultaneous Schur decomposition of several nonsymmetric matrices to achieve automatic pairing in multidimensional harmonic retrieval problems," *IEEE Transactions on Signal Processing*, vol. 46, no. 1, pp. 161–169, January 1998.

[18] A.-J. van der Veen, M. C. Vanderveen, and A. Paulraj, "Joint angle and delay estimation using shift-invariance techniques," *IEEE Transactions on Signal Processing*, vol. 46, no. 2, pp. 405–418, February 1998.

[19] H. Zhang, S. Venkateswaran, and U. Madhow, "Channel modeling and mimo capacity for outdoor millimeter wave links," in *2010 IEEE Wireless Communications and Networking Conference (WCNC)*, 2010, pp. 1–6.

[20] S. Hur, T. Kim, D. J. Love, J. V. Krogmeier, T. A. Thomas, and A. Ghosh, "Multilevel millimeter wave beamforming for wireless backhaul," in *2011 IEEE GLOBECOM Workshops (GC Wkshps)*, 2011, pp. 253–257.

[21] M. C. Vanderveen, A.-J. Van der Veen, and A. Paulraj, "Estimation of multipath parameters in wireless communications," *IEEE Transactions on Signal Processing*, vol. 46, no. 3, pp. 682–690, 1998.

[22] A. Wang, L. Liu, and J. Zhang, "Low Complexity Direction of Arrival (DoA) Esitmation for 2D Massive MIMO Systems," in *IEEE GLOBECOM Workshop on Emerging Technologies for LTE-Advanced and Beyond-4G*, December 2012.

[23] H. Lev-Ari *et al.*, "Efficient solution of linear matrix equations with application to multistatic antenna array processing," *Communications in Information & Systems*, vol. 5, no. 1, pp. 123–130, 2005.

[24] A.-J. Van der Veen, M. C. Vanderveen, and A. Paulraj, "Joint angle and delay estimation using shift-invariance techniques," *IEEE Transactions on Signal Processing*, vol. 46, no. 2, pp. 405–418, 1998.

[25] Y.-H. Nam, M. S. Rahman, Y. Li, G. Xu, E. Onggosanusi, J. Zhang, and J.-Y. Seol, "Full dimension mimo for lte-advanced and 5g," in *2015 Information Theory and Applications Workshop*, Febuary 2015.

[26] I. Tzanidis, Y. Li, G. Xu, J.-Y. Seol, J. C. Zhang, I. S. Team, and D. Samsung, "2d active antenna array design for fd-mimo system and antenna virtualization techniques," *International Journal of Antennas and Propagation*, 2015.

[27] L. Cheng, Y.-c. Wu, J. C. Zhang, and L. Liu, "Subspace identification for doa estimation in massive/full-dimension mimo system: Bad data mitigation and automatic source enumeration," *IEEE Transactions on Signal Processing*, vol. 63, no. 22, pp. 5897–5909, July 2015.

[28] S. Noh, M. D. Zoltowski, Y. Sung, and D. J. Love, "Pilot beam pattern design for channel estimation in massive mimo systems," *IEEE Journal of Selected Topics in Signal Processing*, vol. 8, no. 5, pp. 787–801, 2014.

[29] H. Wang, Z. Pan, J. Ni, and I. Chih-Lin, "A spatial domain based method against pilot contamination for multi-cell massive mimo systems," in *2013 8th International ICST Conference on Communications and Networking in China (CHINACOM)*, 2013, pp. 218–222.

[30] O. El Ayach, S. Rajagopal, S. Abu-Surra, Z. Pi, and R. W. Heath, "Spatially sparse precoding in millimeter wave mimo systems," *IEEE Transactions on Wireless Communications*, vol. 13, no. 3, pp. 1499–1513, 2014.

[31] L. Liu, Y. Li, and J. Zhang, "Doa estimation and achievable rate analysis for 3d millimeter wave massive mimo systems," in *2014 IEEE 15th International Workshop on Signal Processing Advances in Wireless Communications (SPAWC)*. IEEE, June 2014, pp. 6–10.

Appendix A

Proof of Theorem 1

The first order approximation of the MSE for the time frequency using unitary ESPRIT is given by (3.12):

$$\mathbb{E}\left\{(\triangle w_\ell)^2\right\} = \frac{1}{2}\left(\mathbf{r}_\ell^H \cdot \mathbf{W}_{mat}^* \cdot \mathbf{R}_{nn}^{(fba)T} \cdot \mathbf{W}_{mat}^T \cdot \mathbf{r}_\ell - \mathrm{Re}\left\{\mathbf{r}_\ell^T \cdot \mathbf{W}_{mat} \cdot \mathbf{C}_{nn}^{(fba)} \cdot \mathbf{W}_{mat}^T \cdot \mathbf{r}_\ell\right\}\right). \tag{A.1}$$

The vector $\mathbf{r}_\ell$ and the matrix $\mathbf{W}_{mat}$ are given by

$$\mathbf{r}_\ell = \mathbf{q}_\ell \otimes \left(\left[(\mathbf{J}_1\mathbf{U}_s)^\dagger \left(\mathbf{J}_2/e^{j\cdot w_\ell} - \mathbf{J}_1\right)\right]^T \mathbf{p}_\ell\right) \tag{A.2}$$

$$\mathbf{W}_{mat} = \left(\mathbf{\Sigma}_s^{-1}\mathbf{V}_s^T\right) \otimes \left(\mathbf{U}_n\mathbf{U}_n^H\right), \tag{A.3}$$

Denote $\boldsymbol{\beta}_\ell = \mathbf{V}_s\mathbf{\Sigma}_s^{-1}\mathbf{q}_\ell$ and $\boldsymbol{\alpha}_\ell = \left(\mathbf{p}_\ell^T (\mathbf{J}_1\mathbf{U}_s)^\dagger \left(\mathbf{J}_2/e^{jw_\ell} - \mathbf{J}_1\right)\left(\mathbf{U}_n\mathbf{U}_n^H\right)\right)^T$, we have

$$\begin{aligned}
\mathbf{W}_{mat}^T\mathbf{r}_\ell &= \left(\left(\mathbf{\Sigma}_s^{-1}\mathbf{V}_s^T\right) \otimes \left(\mathbf{U}_n\mathbf{U}_n^H\right)\right)^T \left(\mathbf{q}_\ell \otimes \left(\left[(\mathbf{J}_1\mathbf{U}_s)^\dagger \left(\mathbf{J}_2/e^{j\cdot w_\ell} - \mathbf{J}_1\right)\right]^T \mathbf{p}_\ell\right)\right) \\
&= \left(\mathbf{V}_s\mathbf{\Sigma}_s^{-1}\mathbf{q}_\ell\right) \otimes \left(\mathbf{p}_\ell^T (\mathbf{J}_1\mathbf{U}_s)^\dagger \left(\mathbf{J}_2/e^{jw_\ell} - \mathbf{J}_1\right)\left(\mathbf{U}_n\mathbf{U}_n^H\right)\right)^T \\
&= \boldsymbol{\beta}_\ell \otimes \boldsymbol{\alpha}_\ell
\end{aligned}$$

The MSE in (A.1) can be rewritten as:

$$\mathbb{E}\left\{(\triangle w_\ell)^2\right\} = \frac{1}{2}\left((\boldsymbol{\beta}_\ell \otimes \boldsymbol{\alpha}_\ell)^H \cdot \mathbf{R}_{nn}^{(fba)T} \cdot (\boldsymbol{\beta}_\ell \otimes \boldsymbol{\alpha}_\ell) - \mathrm{Re}\left\{(\boldsymbol{\beta}_\ell \otimes \boldsymbol{\alpha}_\ell)^T \cdot \mathbf{C}_{nn}^{(fba)} (\boldsymbol{\beta}_\ell \otimes \boldsymbol{\alpha}_\ell)\right\}\right). \tag{A.4}$$

The covariance and complementary covariance matrix in (A.4) are shown in (2.7):

$$\mathbf{R}_{nn}^{(fba)} = \begin{bmatrix} \mathbf{R}_{nn} & \mathbf{0} \\ \mathbf{0} & \boldsymbol{\Pi}_{LWMN}\mathbf{R}_{nn}^{*}\boldsymbol{\Pi}_{LWMN} \end{bmatrix}$$
$$\mathbf{C}_{nn}^{(fba)} = \begin{bmatrix} \mathbf{0} & \mathbf{R}_{nn}\boldsymbol{\Pi}_{LWMN} \\ \boldsymbol{\Pi}_{LWMN}\mathbf{R}_{nn}^{*} & \mathbf{0} \end{bmatrix}.$$

We first need to simplify $\mathbf{R}_{nn}^{(fba)}$ and $\mathbf{C}_{nn}^{(fba)}$ based on **Lemma** 1:

$$\begin{aligned} \boldsymbol{\Pi}_{MNLW}\mathbf{R}_{nn}\boldsymbol{\Pi}_{MNLW} &= (\boldsymbol{\Pi}_{MN} \otimes \boldsymbol{\Pi}_{LW})\left(\sigma^2\mathbf{I}_{MN} \otimes \mathbf{G}\right)(\boldsymbol{\Pi}_{MN} \otimes \boldsymbol{\Pi}_{LW}) \\ &= \sigma^2\left(\boldsymbol{\Pi}_{MN}\boldsymbol{\Pi}_{MN}\boldsymbol{\Pi}_{MN}\right) \otimes \left(\boldsymbol{\Pi}_{LW}\mathbf{G}\boldsymbol{\Pi}_{LW}\right) \\ &= \sigma^2\mathbf{I}_{MN} \otimes \mathbf{G}_g^{'} \end{aligned} \tag{A.5}$$

$$\begin{aligned} \mathbf{R}_{nn}\boldsymbol{\Pi}_{MNLW} &= \left(\sigma^2\mathbf{I}_{MN} \otimes \mathbf{G}\right)(\boldsymbol{\Pi}_{MN} \otimes \boldsymbol{\Pi}_{LW}) \\ &= \sigma^2\boldsymbol{\Pi}_{MN} \otimes (\mathbf{G}_g\boldsymbol{\Pi}_{LW}) \end{aligned} \tag{A.6}$$

$$\begin{aligned} \boldsymbol{\Pi}_{MNLW}\mathbf{R}_{nn} &= (\boldsymbol{\Pi}_{MN} \otimes \boldsymbol{\Pi}_{LW})\left(\sigma^2\mathbf{I}_M N \otimes \mathbf{G}\right) \\ &= \sigma^2\boldsymbol{\Pi}_{MN} \otimes (\boldsymbol{\Pi}_{LW}\mathbf{G}_g), \end{aligned} \tag{A.7}$$

where $\mathbf{G}_g^{'} = \mathrm{diag}\left\{\left[|\mathbf{g}_F(\lfloor\frac{LW}{2}\rfloor)|^{-2}, \ldots, |\mathbf{g}_F(-\lceil\frac{LW}{2}\rceil)|^{-2}\right]\right\}$.

The vector $\boldsymbol{\alpha}_\ell$ can be simplified as [15]:

$$\begin{aligned} \boldsymbol{\alpha}_\ell^T &= \mathbf{p}_\ell^T\left(\mathbf{J}_1\mathbf{U}_s\right)^\dagger\left(\mathbf{J}_2/e^{jw_\ell} - \mathbf{J}_1\right)\left(\mathbf{U}_n\mathbf{U}_n^H\right) \\ &= \mathbf{e}_\ell^T\left(\left(\mathbf{J}_2\mathbf{F}_w^T\right)^\dagger\mathbf{J}_2 - \left(\mathbf{J}_1\mathbf{F}_w^T\right)^\dagger\mathbf{J}_1\right), \end{aligned} \tag{A.8}$$

where $\mathbf{e}_\ell = \begin{bmatrix} 0 & \dots & 1 & \dots & 0 \end{bmatrix}$ is the column selection vector with all zeros elements except the ℓ-th one.

According to **Lemma** 3, when the sample number LW is large, we have

$$\begin{aligned} \left(\mathbf{J}_2\mathbf{F}_w^T\right)^\dagger &= \left(\left(\mathbf{J}_2\mathbf{F}_w^T\right)^H\left(\mathbf{J}_2\mathbf{F}_w^T\right)\right)^{-1}\left(\mathbf{J}_2\mathbf{F}_w^T\right)^H \\ &= \frac{1}{LW-1}\left(\frac{\left(\mathbf{J}_2\mathbf{F}_w^T\right)^H\left(\mathbf{J}_2\mathbf{F}_w^T\right)}{LW-1}\right)^{-1}\left(\mathbf{J}_2\mathbf{F}_w^T\right)^H \\ &= \frac{1}{LW-1}\left(\mathbf{J}_2\mathbf{F}_w^T\right)^H. \end{aligned} \tag{A.9}$$

Similarly, we have:

$$\left(\mathbf{J}_1\mathbf{F}_w^T\right)^\dagger = \frac{1}{LW-1}\left(\mathbf{J}_1\mathbf{F}_w^T\right)^H. \tag{A.10}$$

Substitute the preceding results into (A.8), the simplified result of vector $\boldsymbol{\alpha}_\ell^T$ is given by

$$\boldsymbol{\alpha}_\ell^T = \frac{1}{LW-1}\left[-1,0,\dots,0,e^{-j(LW-1)w_\ell}\right]. \tag{A.11}$$

In order to simplify the term $\boldsymbol{\beta}_\ell$, we need to obtain the singular decomposition (SVD) of the noiseless received signal which is processed by forward-backward averaging:

$$\begin{aligned} &\left[\mathbf{F}_w^T\mathrm{diag}\left\{\mathbf{b}\right\}\mathbf{A}^T \quad \boldsymbol{\Pi}_{LW}\mathbf{F}_w^H\left\{\mathrm{diag}\left\{\mathbf{b}\right\}\mathbf{A}^T\right\}^*\boldsymbol{\Pi}_{MN}\right] \\ &= \left[\mathbf{F}_w^T\begin{bmatrix} b_1e^{j\varphi_1} & & \\ & \ddots & \\ & & b_Pe^{j\varphi_P}\end{bmatrix}\mathbf{A}^T \quad \mathbf{F}_w^T\boldsymbol{\Lambda}\left\{\begin{bmatrix} b_1e^{j\varphi_1} & & \\ & \ddots & \\ & & b_Pe^{j\varphi_P}\end{bmatrix}\mathbf{A}^T\right\}^*\boldsymbol{\Pi}_{MN}\right] \\ &= \mathbf{F}_w^T\mathrm{diag}\left\{\mathbf{b}_g\right\}\left[\mathbf{A}_e^T \quad \boldsymbol{\Lambda}\mathbf{A}_e^H\boldsymbol{\Pi}_{MN}\right], \end{aligned}$$

where $\boldsymbol{\Lambda} = \begin{bmatrix} e^{-(LW-1)w_1} & & \\ & \ddots & \\ & & e^{-(LW-1)w_p}\end{bmatrix}$, $\mathbf{b}_g = \begin{bmatrix} b_1 & \dots & b_P\end{bmatrix}$ and $\mathbf{A}_e^T = \begin{bmatrix} e^{j\varphi_1} & & \\ & \ddots & \\ & & e^{j\varphi_P}\end{bmatrix}\mathbf{A}^T$.

Based on **Lemma** 3 and **Lemma** 4, we can obtain $\mathbf{U}_s = 1/\sqrt{LW}\mathbf{F}_w^T$, $\boldsymbol{\Sigma}_s = \sqrt{2MNLW}\mathrm{diag}\left\{\mathbf{b}_g\right\}$

and $\mathbf{V}_s^H = 1/\sqrt{2MN}\left[\mathbf{A}_e^T \quad \mathbf{\Lambda}\mathbf{A}_e^H\mathbf{\Pi}_{MN}\right]$.

In [15], the vector $\boldsymbol{\beta}_\ell$ is given by:

$$\boldsymbol{\beta}_\ell = \mathbf{V}_s\mathbf{\Sigma}_s^{-1}\mathbf{U}_s^H\mathbf{F}_w^T\mathbf{e}_\ell. \tag{A.12}$$

Substitute $\mathbf{U}_s$, $\mathbf{\Sigma}_s$ and $\mathbf{V}_s$ into (A.12), we have

$$\boldsymbol{\beta}_\ell = \frac{1}{|\mathbf{b}(\ell)|\sqrt{2MN}}\mathbf{V}_s\mathbf{e}_\ell. \tag{A.13}$$

Now, we can calculate the MSE in (A.4) term by term. To be specific, the first term in (A.4) can be simplified as follows:

$$\begin{aligned}(\boldsymbol{\beta}_\ell \otimes \boldsymbol{\alpha}_\ell) &= \frac{1}{|\mathbf{b}(\ell)|\sqrt{2MN}}\begin{bmatrix} \left\{\bar{\mathbf{a}}_\ell e^{j\varphi_\ell}\right\}^* \\ \mathbf{\Pi}_{MN}\bar{\mathbf{a}}_\ell e^{j\varphi_\ell}e^{j(LW-1)w_\ell}\end{bmatrix} \otimes \boldsymbol{\alpha}_\ell \\ &= \frac{1}{|\mathbf{b}(\ell)|\sqrt{2MN}}\begin{bmatrix} \left\{\bar{\mathbf{a}}_\ell e^{j\varphi_\ell}\right\}^* \otimes \boldsymbol{\alpha}_\ell \\ \mathbf{\Pi}_{MN}\bar{\mathbf{a}}_\ell e^{j\varphi_\ell}e^{j(LW-1)w_\ell} \otimes \boldsymbol{\alpha}_\ell\end{bmatrix},\end{aligned} \tag{A.14}$$

where $\bar{\mathbf{a}}_\ell = 1/\sqrt{2MN}\mathbf{a}_\ell$. Substitute (A.14) into (A.4), we have

$$\begin{aligned}&(\boldsymbol{\beta}_\ell \otimes \boldsymbol{\alpha}_\ell)^H \cdot \mathbf{R}_{nn}^{(fba)T} \cdot (\boldsymbol{\beta}_\ell \otimes \boldsymbol{\alpha}_\ell) \\ &= \frac{\sigma^2}{2b_\ell^2 MN}\left((\bar{\mathbf{a}}_\ell^* \otimes \boldsymbol{\alpha}_\ell)^H(\mathbf{I}_{MN} \otimes \mathbf{G}_g)(\bar{\mathbf{a}}_\ell^* \otimes \boldsymbol{\alpha}_\ell) + (\mathbf{\Pi}_{MN}\bar{\mathbf{a}}_\ell \otimes \boldsymbol{\alpha}_\ell)^H\left(\mathbf{I}_{MN} \otimes \mathbf{G}_g^{'}\right)(\mathbf{\Pi}_{MN}\bar{\mathbf{a}}_\ell \otimes \boldsymbol{\alpha}_\ell)\right).\end{aligned} \tag{A.15}$$

Consider $(\mathbf{A}\otimes\mathbf{B})(\mathbf{C}\otimes\mathbf{D}) = (\mathbf{AC})\otimes(\mathbf{BD})$, we have

$$(\bar{\mathbf{a}}_\ell^* \otimes \boldsymbol{\alpha}_\ell)^H(\mathbf{I}_{MN} \otimes \mathbf{G}_g)(\bar{\mathbf{a}}_\ell^* \otimes \boldsymbol{\alpha}_\ell) = \frac{|\mathbf{g}_F(-\lceil\frac{LW}{2}\rceil)|^{-2} + |\mathbf{g}_F(\lfloor\frac{LW}{2}\rfloor)|^{-2}}{2(LW-1)^2} \tag{A.16}$$

,

$$(\mathbf{\Pi}_{MN}\bar{\mathbf{a}}_\ell \otimes \boldsymbol{\alpha}_\ell)^H \left(\mathbf{I}_{MN} \otimes \mathbf{G}_g^{'}\right) (\mathbf{\Pi}_{MN}\bar{\mathbf{a}}_\ell \otimes \boldsymbol{\alpha}_\ell) \overset{(a)}{=} \frac{|\mathbf{g}_F(-\lceil \frac{LW}{2} \rceil)|^{-2} + |\mathbf{g}_F(\lfloor \frac{LW}{2} \rfloor)|^{-2}}{2(LW-1)^2}. \tag{A.17}$$

where $\overset{(a)}{=}$ holds due to $\mathbf{\Pi}_{MN}\mathbf{\Pi}_{MN} = \mathbf{I}_{MN}$. Substitute (A.16) and (A.17) into (A.15), finally we have

$$\begin{aligned} &(\boldsymbol{\beta}_\ell \otimes \boldsymbol{\alpha}_\ell)^H \cdot \mathbf{R}_{nn}^{(fba)} \cdot (\boldsymbol{\beta}_\ell \otimes \boldsymbol{\alpha}_\ell) \\ &= \frac{\sigma^2}{2|\mathbf{b}(\ell)|^2 MN} \frac{|\mathbf{g}_F(-\lceil \frac{LW}{2} \rceil)|^{-2} + |\mathbf{g}_F(\lfloor \frac{LW}{2} \rfloor)|^{-2}}{(LW-1)^2}. \end{aligned} \tag{A.18}$$

Next, we will calculate the second term in (A.4), which is related to the complementary of the covariance matrix $\mathbf{C}_{nn}^{(fba)}$:

$$\begin{aligned} &(\boldsymbol{\beta}_\ell \otimes \boldsymbol{\alpha}_\ell)^T \cdot \mathbf{C}_{nn}^{(fba)} (\boldsymbol{\beta}_\ell \otimes \boldsymbol{\alpha}_\ell) \\ &= \Big((\bar{\mathbf{a}}_\ell^* \otimes \boldsymbol{\alpha}_\ell)^T (\mathbf{\Pi}_{MN} \otimes (\mathbf{G}_g \mathbf{\Pi}_{LW})) (\mathbf{\Pi}_{MN}\bar{\mathbf{a}}_\ell \otimes \boldsymbol{\alpha}_\ell) \\ &+ (\mathbf{\Pi}_{MN}\bar{\mathbf{a}}_\ell \otimes \boldsymbol{\alpha}_\ell)^T (\mathbf{\Pi}_{MN} \otimes (\mathbf{\Pi}_{LW}\mathbf{G}_g)) (\bar{\mathbf{a}}_\ell^* \otimes \boldsymbol{\alpha}_\ell) \Big) \frac{e^{j(LW-1)w_\ell}\sigma^2}{2|\mathbf{b}(\ell)|^2 MN} \\ &= -\frac{\sigma^2}{2|\mathbf{b}(\ell)|_\ell^2 MN} \frac{|\mathbf{g}_F(-\lceil \frac{LW}{2} \rceil)|^{-2} + |\mathbf{g}_F(\lfloor \frac{LW}{2} \rfloor)|^{-2}}{(LW-1)^2}. \end{aligned} \tag{A.19}$$

Substitute (A.18) and (A.19) into (A.4), we have

$$\mathbb{E}\left\{(\triangle w_\ell)^2\right\} = \frac{\sigma^2}{2MN|\mathbf{b}(\ell)|^2} \frac{|\mathbf{g}_F(-\lceil \frac{LW}{2} \rceil)|^{-2} + |\mathbf{g}_F(\lfloor \frac{LW}{2} \rfloor)|^{-2}}{(LW-1)^2}. \tag{A.20}$$

Based on Jacobian matrix, we have:

$$\mathbb{E}\left\{(\triangle \tau_\ell)^2\right\} = \frac{L^2}{4\pi^2}\mathbb{E}\left\{(\triangle w_\ell)^2\right\}. \tag{A.21}$$

Substitute (A.21) into (A.20), the proof is finished.

Appendix B

Proof of Theorem 2

The MSE of the spatial frequencies u_ℓ and v_ℓ using unitary ESPRIT can be expressed as

$$\begin{aligned}&\mathbb{E}\left\{(\triangle v_\ell)^2\right\}\\&=\frac{1}{2}\left(\left(\boldsymbol{\alpha}_{v,\ell}\otimes\boldsymbol{\beta}_\ell\right)^H\cdot\mathbf{R}_{nn}^{(fba)T}\cdot\left(\boldsymbol{\alpha}_{v,\ell}\otimes\boldsymbol{\beta}_\ell\right)-\mathrm{Re}\left\{\left(\boldsymbol{\alpha}_{v,\ell}\otimes\boldsymbol{\beta}_\ell\right)^T\cdot\mathbf{C}_{nn}^{(fba)}\left(\boldsymbol{\alpha}_{v,\ell}\otimes\boldsymbol{\beta}_\ell\right)\right\}\right).\end{aligned}\tag{B.1}$$

$$\begin{aligned}&\mathbb{E}\left\{(\triangle u_\ell)^2\right\}\\&=\frac{1}{2}\left(\left(\boldsymbol{\alpha}_{u,\ell}\otimes\boldsymbol{\beta}_\ell\right)^H\cdot\mathbf{R}_{nn}^{(fba)T}\cdot\left(\boldsymbol{\alpha}_{u,\ell}\otimes\boldsymbol{\beta}_\ell\right)-\mathrm{Re}\left\{\left(\boldsymbol{\alpha}_{u,\ell}\otimes\boldsymbol{\beta}_\ell\right)^T\cdot\mathbf{C}_{nn}^{(fba)}\left(\boldsymbol{\alpha}_{u,\ell}\otimes\boldsymbol{\beta}_\ell\right)\right\}\right).\end{aligned}\tag{B.2}$$

The covariance matrix $\mathbf{R}_{nn}^{(fba)}$ and complementary covariance matrix $\mathbf{C}_{nn}^{(fba)}$ are given by:

$$\begin{aligned}\mathbf{R}_{nn}^{(fba)}&=\begin{bmatrix}\mathbf{R}_{nn}&\mathbf{0}\\\mathbf{0}&\boldsymbol{\Pi}_{LWMN}\mathbf{R}_{nn}^{*}\boldsymbol{\Pi}_{LWMN}\end{bmatrix}\\\mathbf{C}_{nn}^{(fba)}&=\begin{bmatrix}\mathbf{0}&\mathbf{R}_{nn}\boldsymbol{\Pi}_{LWMN}\\\boldsymbol{\Pi}_{LWMN}\mathbf{R}_{nn}^{*}&\mathbf{0}\end{bmatrix}.\end{aligned}$$

where $\mathbf{R}_{nn}$ and $\mathbf{C}_{nn}$ are given by **Lemma** 2.

It can be obtained that

$$\begin{aligned}
\mathbf{\Pi}_{MNLW}\mathbf{R}_{nn}\mathbf{\Pi}_{MNLW} &= \sigma^2\mathbf{G}_g^{'}\otimes\mathbf{I}_{MN}\\
\mathbf{R}_{nn}\mathbf{\Pi}_{MNLW} &= \sigma^2\left(\mathbf{G}_g\mathbf{\Pi}_{LW}\right)\otimes\mathbf{\Pi}_{MN}\\
\mathbf{\Pi}_{MNLW}\mathbf{R}_{nn} &= \sigma^2\left(\mathbf{\Pi}_{LW}\mathbf{G}_g\right)\otimes\mathbf{\Pi}_{MN}.
\end{aligned}$$

$\boldsymbol{\alpha}_{v,\ell}$ in (B.1) is given by:

$$\boldsymbol{\alpha}_{v,\ell}^T = \mathbf{e}_\ell^T\left(\left(\tilde{\mathbf{J}}_{v,2}\mathbf{A}\right)^\dagger\tilde{\mathbf{J}}_{v,2} - \left(\tilde{\mathbf{J}}_{v,1}\mathbf{A}\right)^\dagger\tilde{\mathbf{J}}_{v,1}\right) \tag{B.3}$$

where $\tilde{\mathbf{J}}_{v,1} = [\mathbf{I}_{N-1} \quad \mathbf{0}]\otimes\mathbf{I}_M$ and $\tilde{\mathbf{J}}_{v,2} = [\mathbf{0} \quad \mathbf{I}_{N-1}]\otimes\mathbf{I}_M$ are the selection matrix.

In our previous work [31], we have the following results:

$$\begin{aligned}
\left(\tilde{\mathbf{J}}_{v,1}\mathbf{A}\right)^\dagger &= \left(\left(\tilde{\mathbf{J}}_{v,1}\mathbf{A}\right)^H\left(\mathbf{J}_{v,1}\mathbf{A}\right)\right)^{-1}\left(\tilde{\mathbf{J}}_{v,1}\mathbf{A}\right)^H\\
&= \frac{1}{(N-1)M}\left(\frac{\left(\tilde{\mathbf{J}}_{v,1}\mathbf{A}\right)^H\left(\tilde{\mathbf{J}}_{v,1}\mathbf{A}\right)}{(N-1)M}\right)^{-1}\left(\tilde{\mathbf{J}}_{v,1}\mathbf{A}\right)^H\\
&\overset{(a)}{=} \frac{1}{(N-1)M}\left(\tilde{\mathbf{J}}_{v,1}\mathbf{A}\right)^H,
\end{aligned} \tag{B.4}$$

where (a) holds due to **Lemma** 4.

Similarly, we have

$$\left(\tilde{\mathbf{J}}_{v,2}\mathbf{A}\right)^\dagger = \frac{1}{(N-1)M}\left(\tilde{\mathbf{J}}_{v,2}\mathbf{A}\right)^H. \tag{B.5}$$

Substitute $\tilde{\mathbf{J}}_{v,1}$ and $\tilde{\mathbf{J}}_{v,2}$ into (B.4) and (B.5). After some simplifications, we have

$$\begin{aligned}
&\boldsymbol{\alpha}_{v,\ell} = \mathbf{e}_\ell^T\left(\left(\tilde{\mathbf{J}}_{2,v}\mathbf{A}\right)^\dagger\tilde{\mathbf{J}}_{2,v} - \left(\tilde{\mathbf{J}}_{1,v}\mathbf{A}\right)^\dagger\tilde{\mathbf{J}}_{1,v}\right)\\
&= \left[-1 \quad -e^{-ju_\ell} \quad \ldots \quad -e^{-j(M-1)u_\ell} \quad \ldots \quad e^{-j(N-1)v_\ell} \quad \ldots \quad e^{-j((N-1)v_\ell+u_\ell)} \quad e^{-j((N-1)v_\ell+(M-1)u_\ell)}\right].
\end{aligned}$$

Next, we need to perform the SVD of the noiseless signal in (3.19) to obtain $\boldsymbol{\beta}_\ell$:

$$
\begin{aligned}
&[\mathbf{A}\mathrm{diag}\{\mathbf{b}\}\mathbf{F}_w \quad \boldsymbol{\Pi}_{MN}\mathbf{A}^*\{\mathrm{diag}\{\mathbf{b}\}\mathbf{F}_w\}^*\boldsymbol{\Pi}_{LW}] \\
&= \left[\mathbf{A}\begin{bmatrix} b_1e^{j\varphi_1} & & \\ & \ddots & \\ & & b_\ell e^{j\varphi_\ell}\end{bmatrix}\mathbf{F}_w \quad \mathbf{A}\boldsymbol{\Lambda}\left\{\begin{bmatrix} b_1e^{j\varphi_1} & & \\ & \ddots & \\ & & b_\ell e^{j\varphi_\ell}\end{bmatrix}\mathbf{F}_w\right\}^*\boldsymbol{\Pi}_{LW}\right] \\
&= \mathbf{A}\mathrm{diag}\left\{\mathbf{b}_g\right\}[\mathbf{F}_{ew} \quad \boldsymbol{\Lambda}\mathbf{F}_{ew}^*\boldsymbol{\Pi}_{LW}],
\end{aligned}
$$

where $\boldsymbol{\Lambda} = \begin{bmatrix} e^{-j((M-1)u_1+(N-1)v_1)} & & \\ & \ddots & \\ & & e^{-j((M-1)u_P+(N-1)v_P)}\end{bmatrix}$ and

$$\mathbf{F}_{ew} = \begin{bmatrix} e^{j\varphi_1} & & \\ & \ddots & \\ & & e^{j\varphi_\ell}\end{bmatrix}\mathbf{F}_w.$$

Based on **Lemma** 3 and **Lemma** 4, we can obtain $\mathbf{U}_s = 1/\sqrt{MN}\mathbf{A}$, $\boldsymbol{\Sigma}_s = \sqrt{2MNLW}\mathrm{diag}\left\{\mathbf{b}_g\right\}$ and $\mathbf{V}_s^H = 1/\sqrt{2LW}\,[\mathbf{F}_{ew} \quad \boldsymbol{\Lambda}\mathbf{F}_{ew}^*\boldsymbol{\Pi}_{LW}]$.

Substitute $\mathbf{U}_s$, $\boldsymbol{\Sigma}_s$ and $\mathbf{V}_s$ into $\boldsymbol{\beta}_\ell = \mathbf{V}_s\boldsymbol{\Sigma}_s^{-1}\mathbf{U}_s^H\mathbf{A}\mathbf{e}_\ell$, we have

$$\boldsymbol{\beta}_\ell = \frac{1}{|\mathbf{b}(\ell)|\sqrt{2LW}}\mathbf{V}_s\mathbf{e}_\ell. \tag{B.6}$$

The first term in (B.1) can be simplified as follows:

$$
\begin{aligned}
\boldsymbol{\beta}_\ell \otimes \boldsymbol{\alpha}_{v,\ell} &= \frac{1}{|\mathbf{b}(\ell)|\sqrt{2LW}}\begin{bmatrix} \left\{\overline{\mathbf{f}}_\ell e^{j\varphi_\ell}\right\}^* \\ \boldsymbol{\Pi}_{LW}\left\{\overline{\mathbf{f}}_\ell e^{j\varphi_\ell}\right\}e^{j((M-1)u_\ell+(N-1)v_\ell)}\end{bmatrix} \otimes \boldsymbol{\alpha}_{v,\ell} \\
&= \frac{1}{|\mathbf{b}(\ell)|\sqrt{2LW}}\begin{bmatrix} \left\{\overline{\mathbf{f}}_\ell e^{j\varphi_\ell}\right\}^* \otimes \boldsymbol{\alpha}_{v,\ell} \\ \boldsymbol{\Pi}_{LW}\left\{\overline{\mathbf{f}}_\ell e^{j\varphi_\ell}\right\}e^{j((M-1)u_\ell+(N-1)v_\ell)} \otimes \boldsymbol{\alpha}_{v,\ell}\end{bmatrix},
\end{aligned}
\tag{B.7}
$$

where $\overline{\mathbf{f}}_\ell = 1/\sqrt{2LW}\mathbf{f}_\ell$.

Substitute (B.7) into (B.1), we have

$$\begin{aligned}
&(\boldsymbol{\beta}_\ell \otimes \boldsymbol{\alpha}_\ell)^H \cdot \mathbf{R}_{nn}^{(fba)} \cdot (\boldsymbol{\beta}_\ell \otimes \boldsymbol{\alpha}_\ell) \\
&= \frac{\sigma^2}{|\mathbf{b}(\ell)|^2 2LW} \left(\left(\bar{\mathbf{f}}_\ell^* \otimes \boldsymbol{\alpha}_\ell\right)^H (\mathbf{G}_g \otimes \mathbf{I}_{MN}) \left(\bar{\mathbf{f}}_\ell^* \otimes \boldsymbol{\alpha}_\ell\right) \right. \\
&\left. + \left(\boldsymbol{\Pi}_{LW} \bar{\mathbf{f}}_\ell \otimes \boldsymbol{\alpha}_\ell\right)^H \left(\mathbf{G}_g^{'} \otimes \mathbf{I}_{MN}\right) \left(\boldsymbol{\Pi}_{LW} \bar{\mathbf{f}}_\ell \otimes \boldsymbol{\alpha}_\ell\right) \right).
\end{aligned} \tag{B.8}$$

The first term in (B.8) can be simplified as follows:

$$\begin{aligned}
\left(\bar{\mathbf{f}}_\ell^* \otimes \boldsymbol{\alpha}_\ell\right)^H (\mathbf{G}_g \otimes \mathbf{I}_{MN}) \left(\bar{\mathbf{f}}_\ell^* \otimes \boldsymbol{\alpha}_\ell\right) &= \frac{\sum_{i=1}^{LW} |\mathbf{g}_F(i)|^{-2}}{(N-1)^2 M(LW)} \\
\left(\boldsymbol{\Pi}_{MN} \bar{\mathbf{f}}_\ell \otimes \boldsymbol{\alpha}_\ell\right)^H \left(\mathbf{G}_g^{'} \otimes \mathbf{I}_{MN}\right) \left(\boldsymbol{\Pi}_{MN} \bar{\mathbf{f}}_\ell \otimes \boldsymbol{\alpha}_\ell\right) &= \frac{\sum_{i=-\lceil \frac{LW}{2} \rceil}^{\lfloor \frac{LW}{2} \rfloor} |\mathbf{g}_F(i)|^{-2}}{(N-1)^2 M(LW)}.
\end{aligned} \tag{B.9}$$

Substitute (B.9) into (B.8), we have

$$(\boldsymbol{\beta}_\ell \otimes \boldsymbol{\alpha}_\ell)^H \cdot \mathbf{R}_{nn}^{(fba)T} \cdot (\boldsymbol{\beta}_\ell \otimes \boldsymbol{\alpha}_\ell) = \frac{\sigma^2 \sum_{i=-\lceil \frac{LW}{2} \rceil}^{\lfloor \frac{LW}{2} \rfloor} |\mathbf{g}_F(i)|^{-2}}{2|\mathbf{b}(\ell)|^2 (LW)^2 (N-1)^2 M}. \tag{B.10}$$

Similarly, we can get

$$(\boldsymbol{\beta}_\ell \otimes \boldsymbol{\alpha}_\ell)^T \cdot \mathbf{C}_{nn}^{(fba)} \cdot (\boldsymbol{\beta}_\ell \otimes \boldsymbol{\alpha}_\ell) = -\frac{\sigma^2 \sum_{i=-\lceil \frac{LW}{2} \rceil}^{\lfloor \frac{LW}{2} \rfloor} |\mathbf{g}_F(i)|^{-2}}{2|\mathbf{b}(\ell)|^2 (LW)^2 (N-1)^2 M}. \tag{B.11}$$

Substitute (B.9) and (B.10) into (B.1), we have

$$\mathbb{E}\left\{ (\triangle v_\ell)^2 \right\} = \frac{\sigma^2 \sum_{i=-\lceil \frac{LW}{2} \rceil}^{\lfloor \frac{LW}{2} \rfloor} |\mathbf{g}_F(i)|^{-2}}{|\mathbf{b}(\ell)|^2 (LW)^2 (N-1)^2 M}. \tag{B.12}$$

Similarly, we have

$$\mathbb{E}\left\{ (\triangle u_\ell)^2 \right\} = \frac{\sigma^2 \sum_{i=-\lceil \frac{LW}{2} \rceil}^{\lfloor \frac{LW}{2} \rfloor} |\mathbf{g}_F(i)|^{-2}}{|\mathbf{b}(\ell)|^2 (LW)^2 (M-1)^2 N}. \tag{B.13}$$

Based on Jacobian matrix, we have:

$$\begin{aligned}
\mathbb{E}\left\{(\triangle\theta_\ell)^2\right\} &= \mathbb{E}\left\{(\triangle u_\ell)^2\right\}\frac{1}{\pi^2\sin^2(\theta_\ell)} \\
\mathbb{E}\left\{(\triangle\phi_\ell)^2\right\} &= \frac{\mathbb{E}\left\{(\triangle u_\ell)^2\right\}\cot^2(\theta_\ell)\cot^2(\phi_\ell)}{\pi^2\sin^2(\theta_\ell)} + \frac{\mathbb{E}\left\{(\triangle v_\ell)^2\right\}}{\pi^2\sin^2(\theta_\ell)\sin^2(\phi_\ell)}.
\end{aligned} \tag{B.14}$$

Finally, substitute (B.12) and (B.13) into (B.14), we have the desirable results.

Appendix C

Proof of Theorem 3

For the standard ESPRIT method, it is easy to find that the complementary covariance matrix is equal to zero matrix:

$$\mathbf{C}_{nn} = \mathbf{0}.$$

Hence the expression of the MSE using ESPRIT method in (4.8) is reduced to:

$$\mathbb{E}\left\{\left(\triangle\mu_\ell^{(r)}\right)^2\right\} = \frac{1}{2}\left(\mathbf{r}_\ell^{(r)H}\cdot\mathbf{W}_{mat}^{*}\cdot\mathbf{R}_{nn}^{T}\cdot\mathbf{W}_{mat}^{T}\cdot\mathbf{r}_\ell^{(r)}\right). \tag{C.1}$$

where $\mathbf{R}_{nn}$ can be obtained in **Lemma** 5.

Denote $\boldsymbol{\beta}_\ell = \mathbf{V}_s\boldsymbol{\Sigma}_s^{-1}\mathbf{q}_\ell$ and $\boldsymbol{\alpha}_\ell^{(r)} = \left(\mathbf{p}_\ell^T\left(\mathbf{J}_1\mathbf{U}_s\right)^\dagger\left(\mathbf{J}_2/e^{j\mu_\ell^{(r)}} - \mathbf{J}_1\right)\left(\mathbf{U}_n\mathbf{U}_n\right)\right)^T$, we have

$$\mathbf{W}_{mat}^{T}\mathbf{r}_\ell^{(r)} = \boldsymbol{\beta}_\ell \otimes \boldsymbol{\alpha}_\ell^{(r)} \tag{C.2}$$

.

Substitute (4.12) and (C.2) into (C.1) we have

$$\begin{aligned}
&\mathbb{E}\left\{\left(\triangle\mu_\ell^{(r)}\right)^2\right\} = \frac{\sigma^2}{2}\left(\mathbf{r}_\ell^{(r)H}\cdot\mathbf{W}^*\cdot\mathbf{I}_K\otimes\mathbf{G}_g\otimes\mathbf{I}_{MN}\cdot\mathbf{W}^T\cdot\mathbf{r}_\ell^{(r)}\right)\\
&=\frac{\sigma^2}{2}||\mathbf{I}_K\otimes\mathbf{G}_g^{-1/2}\otimes\mathbf{I}_{MN}\cdot\mathbf{W}^T\cdot\mathbf{r}_\ell^{(r)}||_2^2\\
&=\frac{\sigma^2}{2}||\mathbf{I}_K\otimes\mathbf{G}_g^{-1/2}\otimes\mathbf{I}_{MN}\cdot\left(\boldsymbol{\beta}_\ell\otimes\boldsymbol{\alpha}_\ell^{(r)}\right)||_2^2\\
&=\frac{\sigma^2}{2}||\boldsymbol{\beta}_\ell||_2^2\left(\boldsymbol{\alpha}_\ell^{(r)H}\left(\mathbf{G}_g\otimes\mathbf{I}_{MN}\right)\boldsymbol{\alpha}_\ell^{(r)}\right).
\end{aligned} \tag{C.3}$$

It has been proved in [15] that $||\boldsymbol{\beta}_\ell||_2^2 = \mathbf{R}_{ss}^{-1}(\ell,\ell)/K$, where $\mathbf{R}_{ss}$ is the covariance matrix of the transmitted signals, here it denotes the covariance matrix of the channel attenuator:

$$\mathbf{R}_{ss} = \mathbb{E}\left\{\mathbf{b}\mathbf{b}^H\right\}. \tag{C.4}$$

Following the prove of the **Theorem** 2, we can get

$$\begin{aligned}
&\boldsymbol{\alpha}_\ell^{(r)H}\left(\mathbf{G}_g\otimes\mathbf{I}_{MN}\right)\boldsymbol{\alpha}_\ell^{(r)}\\
&=\frac{\left(|\mathbf{g}_F(-\lceil\frac{LW}{2}\rceil)|^{-2}+|\mathbf{g}_F(\lfloor\frac{LW}{2}\rfloor)|^{-2}\right)M_r}{(M_r-1)^2M_c}.
\end{aligned} \tag{C.5}$$

where $M_1 = LW$, $M_2 = M$, $M_3 = N$ and $M_c = M_1M_2M_3$.

Substitute $||\boldsymbol{\beta}_\ell||_2^2 = \mathbf{R}_{ss}^{-1}(\ell,\ell)/K$ and (C.5) into (C.1), finally, we have

$$\begin{aligned}
&\mathbb{E}\left\{\left(\triangle\mu_\ell^{(r)}\right)^2\right\} = \sigma^2\frac{\mathbf{R}_{ss}^{-1}(\ell,\ell)}{2K}\frac{\left(|\mathbf{g}_F(-\lceil\frac{LW}{2}\rceil)|^{-2}+|\mathbf{g}_F(\lfloor\frac{LW}{2}\rfloor)|^{-2}\right)M_r}{(M_r-1)^2M_c},\\
&\forall r\in\{1,2,3\},\ell\in\{1,2,\ldots,P\}.
\end{aligned} \tag{C.6}$$

Based on (C.6), we can obtain the MSE of the spatial frequencies u_ℓ and v_ℓ as follows:

$$\begin{aligned}\mathbb{E}\left\{(\triangle u_\ell)^2\right\} &= \sigma^2 \frac{\mathbf{R}_{ss}^{-1}(\ell,\ell)}{2K} \frac{\left(|\mathbf{g}_F(-\lceil \frac{LW}{2} \rceil)|^{-2} + |\mathbf{g}_F(\lfloor \frac{LW}{2} \rfloor)|^{-2}\right)}{(M-1)^2 NLW} \\ \mathbb{E}\left\{(\triangle v_\ell)^2\right\} &= \sigma^2 \frac{\mathbf{R}_{ss}^{-1}(\ell,\ell)}{2K} \frac{\left(|\mathbf{g}_F(-\lceil \frac{LW}{2} \rceil)|^{-2} + |\mathbf{g}_F(\lfloor \frac{LW}{2} \rfloor)|^{-2}\right)}{(N-1)^2 MLW}.\end{aligned} \tag{C.7}$$

Substitute (C.7) into (B.14), the proof is finished.